Micrometeorological Methods to Determine Evapotranspiration

Shaomin Liu and Ziwei Xu

Contents

Abstract

Evapotranspiration (ET) is a combination of two distinct processes, soil or water evaporation (E) and plant transpiration (T), that occur between plants and the atmosphere, soil and the atmosphere, and water and the atmosphere. ET is also an important link between the terrestrial ecosystem and hydrological processes. In this chapter, we focus primarily on ET measurements using micrometeorological methods. Three typical ET measurement techniques, namely, the Bowen ratio-energy balance, eddy covariance, and scintillometer methods, which have a long history and are used widely throughout the world, are introduced. A brief review of their theoretical background, installation and maintenance, data processing and quality control, and footprint is presented, in addition to a brief summary of the advantages and disadvantages of each method. Additionally, ET measurements at

S. Liu (✉) · Z. Xu
State Key Laboratory of Earth Surface Processes and Resource Ecology, School of Natural Resources, Faculty of Geographical Science, Beijing Normal University, Beijing, China
e-mail: smliu@bnu.edu.cn

X. Li, H. Vereecken (eds.), *Observation and Measurement of Ecohydrological Processes*, Ecohydrology, https://doi.org/10.1007/978-3-662-48297-1_7

observational networks and intensive experiments are presented. The ET measurement methods differ in observational theory, temporal–spatial scales, and precision. Researchers can select a suitable method according to their research objectives.

Keywords
Evapotranspiration · Bowen ratio-energy balance method · Eddy covariance method · Scintillometer method

Introduction

Several issues, such as a shortage of fresh water resources and deterioration of water quality, have led to a new interdiscipline, eco-hydrology. One of its core research goals is to reveal the factors and regulation mechanisms influencing the change in the ecological environment related to the water cycle. Evapotranspiration (ET) is a combination of two separate processes, soil or water evaporation (E) and plant transpiration (T), that occur between plants and the atmosphere, soil and the atmosphere, and water and the atmosphere. ET is an essential component of energy and water budgets and is an important process in the soil-plant-atmosphere continuum (SPAC), the water and energy source for crop growth, and an important link between terrestrial ecosystems and hydrological processes. Some important ecosystem parameters and processes, such as soil moisture, vegetation productivity, ecosystem energy, water, and nutrient budgets, are influenced by ET (Wever et al. 2002).

ET measurements have been performed for more than 300 years throughout the world. The first lysimeter to study water use can trace its history back to the seventeenth century (Howell et al. 1991), and the first self-recording lysimeter was developed in Ohio, USA, in 1937 (Garstka 1937). The Bowen ratio-energy balance method (Bowen 1926) and aerodynamics method (Thornthwaite and Holzman 1939) were subsequently developed. Swinbank (1951) proposed the eddy covariance method to directly measure ET, which is currently widely used around the world. The zero-flux plane (ZFP) method was originally used to calculate the infiltration of soil moisture and has been used to measure ET since the 1970s (Cooper 1979). The scintillometer technique to measure surface fluxes was proposed in the 1970s (Wang et al. 1978), and it has been widely used in land surface process experiments since the 1990s. In addition, quick-weighting (checking the weight quickly by two times under no wind condition and recording the water loss of the whole or part of plant and then calculating the transpiration rate), ventilated chambers, and several thermal-based methods (e.g., packaged and probe sap flow) have been used to obtain quantitative estimates of whole-plant water use since the mid-1930s (Wullschleger et al. 1998; Allen et al. 2011).

Evapotranspiration is not easy to measure due to the numerous influencing factors. The methods used to measure ET are based on different measuring principles, for example, hydrological approaches (such as lysimeter and ZFP), plant

physiological approaches (e.g., quick-weighting, chambers system, and sap flow method), and micrometeorological methods (e.g., Bowen ratio-energy balance, aerodynamics, eddy covariance, and scintillometer). In the hydrological approaches (lysimeter and ZFP), the water balance equation is the basic equation used to estimate ET by determining all other components. The lysimeter method can derive reliable ET estimates with well-defined surfaces and controlling the lower boundary conditions. The main disadvantages of the lysimeter are construction and maintenance and its limited areal extent especially when the surrounding crops are not uniform. The ZFP method relies on locating a plane of zero hydraulic gradient in the soil profile. However, the disadvantage of the ZFP method is that it cannot be used in areas with high precipitation, i.e., where the zero-flux plane is not stable (Khalil et al. 2003). The plant physiology approaches, such as quick-weighting, ventilated chambers, and sap flow methods, can measure one component of ET (transpiration), and they can be used in complex terrain and spatially heterogeneous environments. However, the quick-weighting method cannot obtain continuous data, and it is a destructive measurement; the chambers method creates an artificial environment and is characterized by technical difficulties, especially when measuring high flow flux rates (Dragoni et al. 2005). Radial gradients in sapwood can result in errors in the sap flow method and require scaling procedures to extrapolate from individual trees (Wilson et al. 2001). Micrometeorological methods are widely used to determine ET and energy partitioning in a number of ecosystems. In this chapter, we focus on these types of approach, including the Bowen ratio-energy balance, eddy covariance, and scintillometer methods.

Micrometeorological Methods to Measure Evapotranspiration

Bowen Ratio-Energy Balance Method

The Bowen ratio-energy balance (BREB) is a micrometeorological method based on the energy balance equation that measures two-layer gradients in the collocated air temperature and vapor pressure in the near-surface layer above the evaporating surface (Bowen 1926). This method is often used to estimate the sensible and latent heat flux because of its simplicity, robustness, and low cost. This method also compares favorably with other methods, such as the weighing lysimeters (Prueger et al. 1997), eddy covariance (Cellier and Olioso 1993), and water balance methods (Malek and Bingham 1993).

Theory

The BREB method estimates sensible and latent heat flux from a surface based on measurements of air temperature and humidity gradients, net radiation, and soil heat flux (Fritschen and Simpson 1989).

The sensible heat (H) and latent heat (LE) flux in one-dimension can be described in terms of flux–gradient relationships:

$$H = -\rho c_p k_h \frac{\partial T}{\partial z} \tag{1}$$

$$LE = -\frac{\rho c_p}{\gamma} k_v \frac{\partial e}{\partial z} \tag{2}$$

where ρ is the air density (kg m^{-3}); c_p is the heat capacity of air at a constant pressure (J kg^{-1} °C^{-1}); k_h and k_v are the turbulent transfer coefficients for heat and water vapor (m^2 s^{-1}), respectively; T is the air temperature (°C); e is the actual vapor pressure (kPa); and γ is the psychrometric constant (kPa °C^{-1}).

By assuming $k_h = k_v$ (Verma et al. 1978) and measuring the temperature and vapor pressure gradients between two levels within the constant-flux layer, β is obtained as:

$$\beta = \frac{H}{LE} = \gamma \frac{\partial T/\partial z}{\partial e/\partial z} = \gamma \frac{\Delta T}{\Delta e} \tag{3}$$

where ΔT and Δe are the temperature (°C) and vapor pressure (kPa) differences between the two measurement levels, respectively.

The energy balance equation is usually expressed as:

$$R_n = H + LE + G_0 \tag{4}$$

where R_n is the net radiation (W m^{-2}), and G_0 is the surface soil heat flux (W m^{-2}). The sensible heat and latent heat flux can be derived by combining Eqs. 3 and 4.

$$H = \frac{\beta}{1+\beta}(R_n - G_0) \tag{5}$$

$$LE = \frac{R_n - G_0}{1+\beta} \tag{6}$$

The BREB method relies on several assumptions (Fritschen and Simpson 1989). Transport is assumed to be one-dimensional, with no horizontal gradients. The sensors that measure gradients are assumed to be located within the constant-flux layer, where fluxes are assumed to be constant with height. The surface is assumed to be homogeneous with respect to heat sources and sinks, water vapor, and momentum. The ratio of the turbulent transfer coefficients for heat (k_h) and water vapor (k_v) is assumed to be 1.

Installation and Maintenance

BREB system is composed of air temperature and humidity sensors to measure gradients, a radiometer (net radiometer or four-component radiometer), soil heat flux plates, and soil temperature and moisture sensors in the near-surface layer. To reduce the observed errors, the sensors must maintain high sensitivity and precision, especially the air temperature and humidity sensors. Generally, BREB systems can

Fig. 1 BREB systems. (**a**) Normal, (**b**) interchange, and (**c**) pumping

be categorized as normal (two layers of air temperature and humidity observations in a fixed position), interchange (two layers of air temperature and humidity sensors interchanged in a period), and pumping (water vapor was pumped in the two layers of the channels to a gas analyzer (i.e., Li 840) and then analyzed) (Payero et al. 2003; Fritschen and Fritschen 2005; Allen et al. 2011) (Fig. 1).

When the BREB system is used in an experiment, it must be installed in the downwind of the surfaces of interest. The two layers of air temperature and humidity sensors must maintain a certain height distance to ensure that the differences in temperature and humidity are greater than their accuracy. The lower sensor should be at least 0.3 m above the crop canopy for relatively homogeneous surfaces, and the upper sensor should be 1–2 m above the lower sensor (Allen et al. 2011). The sampling interval is usually 10 s or less, and data are typical stored every 15 min (for the interchange type) or 30 min (for the normal and pumping type). Half-hourly values are calculated as the average of two corresponding 15-min periods (for the interchange type). The net radiometer, soil heat flux plate, and soil temperature and moisture measurements are recorded every 10 s, and the average values are calculated and registered every 30 min.

Sensor drift, calibration errors, and environmental effects may cause errors in the air temperature and vapor pressure gradients when using the BREB method. When the gradients are small, the errors become significant and may even change the sign of the observed fluxes. To obtain valid air temperature and vapor pressure gradients, it is essential to periodically switch the locations of the upper and lower sensors using an automatic exchange mechanism. When an exchange mechanism is used, the sensors can be exchanged periodically, for example, every 15 min. After each exchange, sampling must stop for a period to allow the sensors to equilibrate to the conditions of the new location (Fritschen and Fritschen 2005).

The BREB system is closely supervised, and general maintenance is performed at least once a month. Maintenance includes cleaning and adjusting the heights of the

lower and upper Bowen ratio arms in response to increased crop height. For the pumping type, the air intake filters must be regularly cleaned or changed. In addition, the net radiometer maintenance includes cleaning the domes, checking the desiccant, and making sure it is properly leveled.

Data Processing and Quality Control

The BREB method is an indirect method compared to methods such as eddy covariance system or lysimeter (Todd et al. 2000), and it also relies on several assumptions. Therefore, the data processing and quality control must be carefully implemented.

First, the quality of R_n should be assured. Current radiometers have high precision; it is important that the radiometer observations represent the average surface conditions similar to that of the source area (the primary contribution of the upwind area to the observed values) of the flux measurement as closely as possible. Second, the soil heat flux must be corrected to the surface. The soil heat plate is usually buried a few centimeters under the soil, and the measurements must be corrected to the surface. There are several correction methods, including Plate Cal (combination of heat flux plate measurements and calorimetry), TCAV (averaging soil thermocouple probe), TDEC (thermal diffusion equation and correction), and HM (harmonic analysis method) (Heusinkverld et al. 2004; Liebethal et al. 2005; Yang and Wang 2008). A suitable method can be selected according to the observation conditions.

The accuracy of the observed latent and sensible heat fluxes depends on the accuracy of the Bowen ratio. In many works, data within the instrumental error of the Bowen ratio system are excluded to avoid serious errors in the flux measurements. For example, the temperature and humidity gradients should be greater than the resolution of the sensors (Perez et al. 1999). For cases in which the β values are close to -1, some authors eliminate values less than -0.75 or values in the range $-1.3 < \beta < -0.7$ (Unland et al. 1996). After careful analysis and deduction, Perez et al. (1999) proposed the following to be satisfied by the BREB method under non-advective conditions (Table 1).

Footprint

The footprint of a measurement is the transfer function between the measured value and the set of forcings on the surface–atmosphere interface, while the source area (the upwind area with the primary contribution to the measurement) can be interpreted as the integral of the footprint function over a specified domain (Schmid 1994, 2002) (Fig. 2). The size and extent of source area depend on many factors, such as the measurement height, atmospheric stability, wind speed and direction, and surface roughness length.

The measurement scales of R_n, G_0, H, and LE are different. The source area of H and LE is on the scale of a hundred meters, and the accuracy relies on the representativeness of the R_n and G_0 measurements.

The observation area of G_0 is limited to a few square meters. Therefore, several sampling sites may be required to represent the area sensed by the other sensors, especially if the surface is heterogeneous. Net radiometers have an observation area

Table 1 Requirements to be satisfied by the BREB method under non-advective conditions

Available energy	Vapor pressure difference	Bowen ratio	Heat fluxes
$R_n - G_0 > 0$	$\Delta e > 0$	$\beta > -1$	$LE > 0$ and $H \leq 0$ for $-1 < \beta \leq 0$ or $H > 0$ for $\beta > 0$
	$\Delta e < 0$	$\beta < -1$	$LE < 0$ and $H > 0$
$R_n - G_0 < 0$	$\Delta e > 0$	$\beta < -1$	$LE > 0$ and $H < 0$
	$\Delta e < 0$	$\beta > -1$	$LE < 0$ and $H \geq 0$ for $-1 < \beta \leq 0$ or $H < 0$ for $\beta > 0$

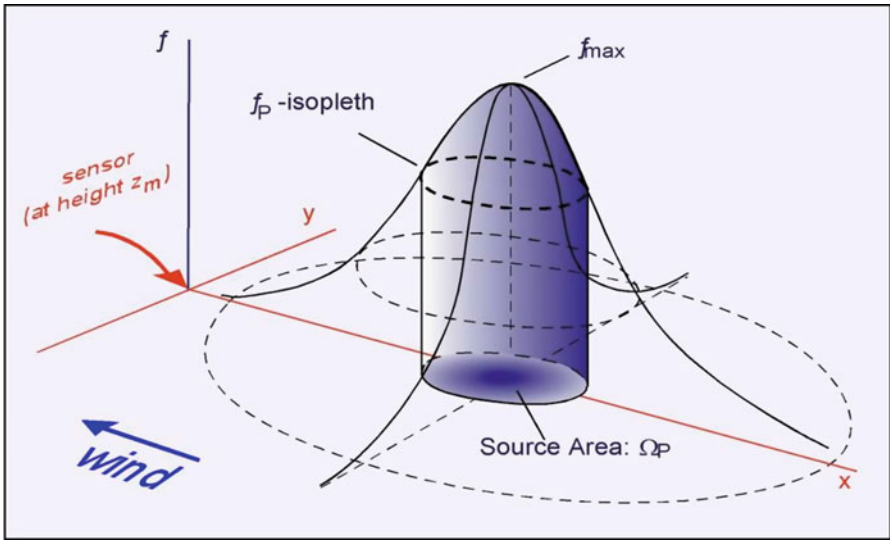

Fig. 2 The source area and its relation to the footprint function (From Schmid 1994)

on the scale of dozens of meters, representing the underlying surface conditions, and they also require more sampling observations for heterogeneous surfaces.

Under homogeneous conditions, the ratio of the source area to the upper measurement height is on the order of 1:100 for the BREB method (Horst and Weil 1992). Fritschen et al. (1983) found that a ratio (fetch/observation height) of 85 was adequate over irrigated cotton with an upwind desert surface. Heilman et al. (1989) reported BREB measurements with a fetch to height ratio of 15 over 0.03 m Bermuda grass with upwind cotton. Stannard (1997) proposed a theoretical model to determine the Bowen ratio fetch and tested it on a Bermuda grass surface.

Summary

Valid Bowen ratio data require careful instrument location, installation, and on-site supervision (Payero et al. 2003). This method assumes that the turbulent transfer coefficients for heat and water vapor are identical, neglecting the heat storage and

advection, and that the surface energy is balanced, which is true in neutral conditions but may not be valid in strongly stable or unstable conditions and when advection appears under heterogeneous surfaces (Cellier and Brunet 1992; Perez et al. 1999).

The BREB method has several advantages and disadvantages (Todd et al. 2000). Its advantages include that it is based on straightforward, simple measurements, it requires no information about the aerodynamic characteristics of the interested surface, it can integrate latent heat fluxes over large areas (scale of hundreds of meters), it can observe fluxes on fine time scales (e.g., 10 min and 30 min), and it can provide continuous, unattended measurements. The disadvantages include sensitivity to the biases of the instruments that measure the gradients and energy balance terms, the possibility of discontinuous data when the Bowen ratio approaches -1, the heavy reliance of the ET observation on the accuracy and representativeness of the R_n and G_0 measurements, and the requirement for an adequate upwind source area to establish an equilibrium boundary layer where the temperature and vapor gradients are constant in horizontal space.

Eddy Covariance Method

The eddy covariance method can observe surface exchanges of momentum, energy, and mass. It is based on the Reynolds decomposition concept, and such exchanges can be derived from the high-frequency fluctuation of three-dimensional velocity, temperature, water vapor, carbon dioxide, etc. Due to the relative robustness of both its theoretical underpinnings and modern environmental sensors, the eddy covariance is widely used to measure vertical turbulent fluxes of energy, water, and CO_2 over various terrestrial ecosystems. Eddy covariance provides a direct measure of flux and enables near continuous coverage over time. Furthermore, it is the predominant method in FLUXNET, the cornerstone for nearly all networks.

Theory

The theoretical basis of the eddy covariance (EC) method, i.e., Reynolds decomposition to separate a quantity into the average and fluctuating parts, was established as early as the year 1895. In 1938, Taylor's frozen turbulence hypothesis (Taylor 1938) was proposed, assuming that the measured changes in time at a point were the result of a frozen turbulence field passing by, which enables derivation of the spatial pattern of turbulence according to its temporal description. Turbulent flux determination based on the EC method was first proposed in the 1950s (Swinbank 1951; Foken 2008). However, the deficiency of observation instruments restricted the development and application of the EC method. The possibility of continuous eddy flux measurements arose in the 1990s with the development of a new generation of sonic anemometers and infrared gas analyzers for water vapor and carbon dioxide (Foken and Oncley 1995). The EC method is based on the transfer equations for momentum, heat, humidity, and trace gases.

Based on the mass conservation equation and Reynolds decomposition, neglecting the horizontal turbulent flux divergence terms and the horizontal variation

of the vertical flux, applying continuity, and assuming a horizontally homogeneous concentration gradient (Feigenwinter et al. 2004), the equation is:

$$\int_0^{z_r} S(t,z)dz = \underbrace{\int_0^{z_r} \frac{\partial \overline{c}(z)}{\partial t} dz}_{I} + \underbrace{\overline{w'c'}(z_r)}_{II} + \underbrace{\int_0^{z_r} \overline{w}(z) \frac{\partial \overline{c}(z)}{\partial z} dz}_{III} + \underbrace{\int_0^{z_r} \left(\overline{u}(z) \frac{\partial \overline{c}(z)}{\partial x} + \overline{v}(z) \frac{\partial \overline{c}(z)}{\partial y} \right) dz}_{IV} \tag{7}$$

where S is the source/sink strength term; u, v, and w are the wind velocity components (m s^{-1}); c is a scalar; x, y, and z are the coordinate system; and z_r is a control volume of height (m). Term I is the storage change, II is the turbulent vertical flux, III is the vertical advection, and IV is the horizontal advection. The overbar represents the Reynolds averaging operator.

Under the assumptions of (1) fully developed turbulence, (2) stationary state, (3) horizontal homogeneity (no advection), (4) constant-flux surface layer, (5) all scales of turbulence being included, and (6) representative to the specific surface, the equation can be simplified as:

$$\int_0^{z_r} S(t,z)dz = \overline{w'c'}(z_r) \tag{8}$$

The sensible heat (H), latent heat (LE), and carbon dioxide (F_c) fluxes are then:

$$H = \rho C_p \overline{w'T'} \tag{9}$$

$$LE = \lambda \overline{w'q'} \tag{10}$$

$$F_c = \overline{w'\mathrm{CO_2}'} \tag{11}$$

where ρ is the air density (kg m^{-3}), c_p is the heat capacity of air at a constant pressure (J kg^{-1} $°C^{-1}$), λ is the latent heat of vaporization for water (J kg^{-1}), T is the air temperature (°C), q is the water vapor density (g m^{-3}), and CO_2 is the carbon dioxide concentration (mg m^{-3}).

Installation and Maintenance

Eddy covariance systems (EC) usually consist of a three-dimensional sonic anemometer that measures wind speed fluctuations in three directions and virtual temperature and an infrared gas analyzer (IRGA) that measures CO_2 and water vapor density fluctuations. The most common sonic anemometers are CSAT3 (Campbell, USA) and WindMaster/R3/HS (Gill, UK); the most common types of IRGA are Li7500/Li7500A/Li7500RS/Li7700 (CH4 analyzer) (LI-COR, USA)/EC150 (Campbell, USA) for open path, Li7200RS (LI-COR, USA) and EC155 (Campbell, USA) for enclosed path, and the integrated CO_2 and H_2O open-path gas analyzer and sonic anemometer IRGASON (Campbell, USA) (Fig. 3).

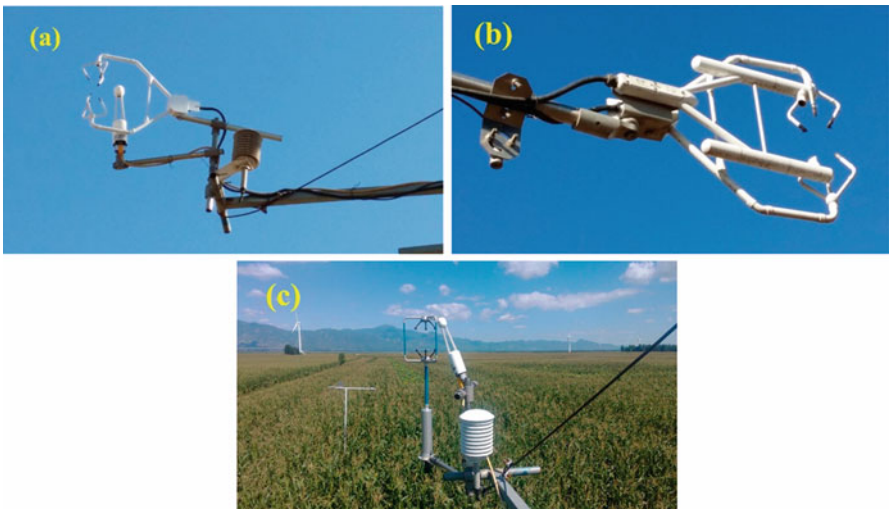

Fig. 3 Eddy covariance system. (**a**) CSAT3 and Li7500A, (**b**) CSAT3 and EC150, and (**c**) Gill and Li7500A

The choice of observation site is very important because it affects the quality of the observed data. Site selection mainly depends on the specific scientific issue of interest. Generally, the selected site should maintain the same prevailing wind direction from the surface of interest during the observation period. Therefore, the prevailing wind direction should be determined before installing the instruments. When the prevailing wind direction is not clear, a common approach is to install the instrument in the center of study area, especially when the surface is homogeneous. Once the observational object is ascertained, the flux tower should be placed in a location that is disturbed by the nearby ecosystem as minimally as possible. The installed height of the EC system is determined according to the research objective and is usually installed at least above 1.5 m or more above the surface or canopy. The sonic anemometer should be aligned to the prevailing wind direction. If the EC system is installed on the tower, the arm length should be two times larger than the tower structure (i.e., the diameter of the tower) to reduce the influence of the tower on the flow distribution. The IRGA sensor should be installed near the sonic anemometer (usually within 20 cm) and slanted a certain angle (15–30°) horizontally.

The raw data for the EC system are high-frequency data (usually 10–20 Hz). The datalogger can store the raw 10-Hz or 20-Hz data (for post-processing) and can process the data into a flux file (usually 30-min period). The raw data (10-Hz or 20-Hz) and flux file can be stored in the datalogger using a CF card. The flux file can be transferred to the researcher via a wireless network (GPRS) in real time so that the data can be regularly checked. The sonic anemometer should remain level (the horizontal bubble in the center), and the IRGA must be kept clean and be calibrated at least twice a year.

Data Processing and Quality Control

The theory of the EC method is based on a series assumption, and it can usually produce reliable results for uniform, flat surfaces. However, the conditions of stationarity in time and homogeneity in space under which the original theories were established are never fully satisfied in practice (Moncrieff et al. 2004). Therefore, careful data processing and quality assurance are important, challenging issues.

There is no uniform scheme for quality control in eddy covariance measurements (Foken et al. 2004). Common quality control measures for EC data include spike detection, lag correction of H_2O/CO_2 relative to the vertical wind component, sonic virtual temperature correction (Schotanus et al. 1983), rotation coordination using the planar fit method (Wilczak et al. 2001), angle of attack error correction (for the Gill-WindMaster sonic anemometer, Nakai and Shimoyama 2012), corrections for density fluctuation (WPL correction, Webb et al. 1980), and frequency response correction.

In addition to these processing steps, half-hourly flux data are screened according to the following criteria: (i) data are rejected when the sensor is malfunctioning (e.g., when there is a fault diagnostic signal), (ii) data are rejected when precipitation occurs within 1 h before or after collection, (iii) incomplete 30-min data are rejected when the percentage of missing data is greater than 3% in the 30-min raw record, and (iv) data are rejected at night during weak turbulence (using the threshold of friction velocity as the criterion) (Liu et al. 2011, 2013).

To be useful, the final data archive must include the data that passes the quality control verification. Measurements are normally flagged according to an index evaluation system. Foken and Wichura (1996) classified tests as stationary tests and integral turbulence characteristics test and proposed a flag for each 30-min flux data run. Three classes were used in the current research (0, best; 1, medium; and 2, poor quality and discarded).

The EC method suffers from an energy imbalance issue. The sum of turbulent latent and sensible heat flux measured by EC method are usually less than the available energy (net radiation minus soil heat flux). An imbalance of approximately 10–30% is traditionally reported. The underlying cause of the imbalance is attributed to measurement errors, an incompletely considered storage term, mismatch between the scales of the energy balance components, and large eddy transport or secondary circulations not captured by EC. Foken (2008) pointed out that the energy imbalance problem is a scale problem, and Foken et al. (2010) concluded that mesoscale circulations resulting from landscape heterogeneity are likely responsible for the energy imbalance at the tower measurement level. Landscape-level heterogeneity in vegetation and topography can also result in an energy imbalance (Stoy et al. 2013), and the EBR would decrease with increasing land surface heterogeneity. There are general two ways to correct the energy imbalance in EC measurements (Twine et al. 2000): (1) the residual method, which assumes that the sensible heat flux is accurate and attributes the residual energy to the latent heat flux using the energy balance equation, and (2) the Bowen ratio correction method, which recomputed the fluxes according to the Bowen ratio values. Charuchittipan et al. (2014) proposed a new method, named

the buoyancy flux ratio, to correct the energy imbalance, which uses the relative contribution of the sensible heat flux to the buoyancy flux to correct the sensible and latent heat fluxes. Flux measurements via the EC method are also subject to systematic and random errors (Wang et al. 2015). A landmark paper by Lenschow et al. (1994) defined systematic and random errors associated with limited samplings of EC measurements. Subsequently, with the continued extensive use of EC systems, several methods have emerged for flux uncertainty estimation (Mann and Lenschow 1994; Finkelstein and Sims 2001; Hollinger and Richardson 2005). The normalized uncertainties range from 10% for sensible heat to 25–30% for latent heat and carbon dioxide fluxes (Finkelstein and Sims 2001).

In long-term observations, missing data will occur due to instrument malfunction, poor maintenance, and bad weather conditions, as well as rejected bad data. In order to obtain continuous ET or carbon measurements, a suitable gap-filling method should be used. Several gap-filling methods are used to complete flux measurement data, such as look-up table (LUT), mean diurnal variations (MDV), nonlinear regression (Regr.), artificial neural networks (ANNs), the Kalman filter (KF), and multiple imputation (MI) (Falge et al. 2001; Hui et al. 2004; Alavi et al. 2006). The general EC data processing flowchart is shown in Fig. 4.

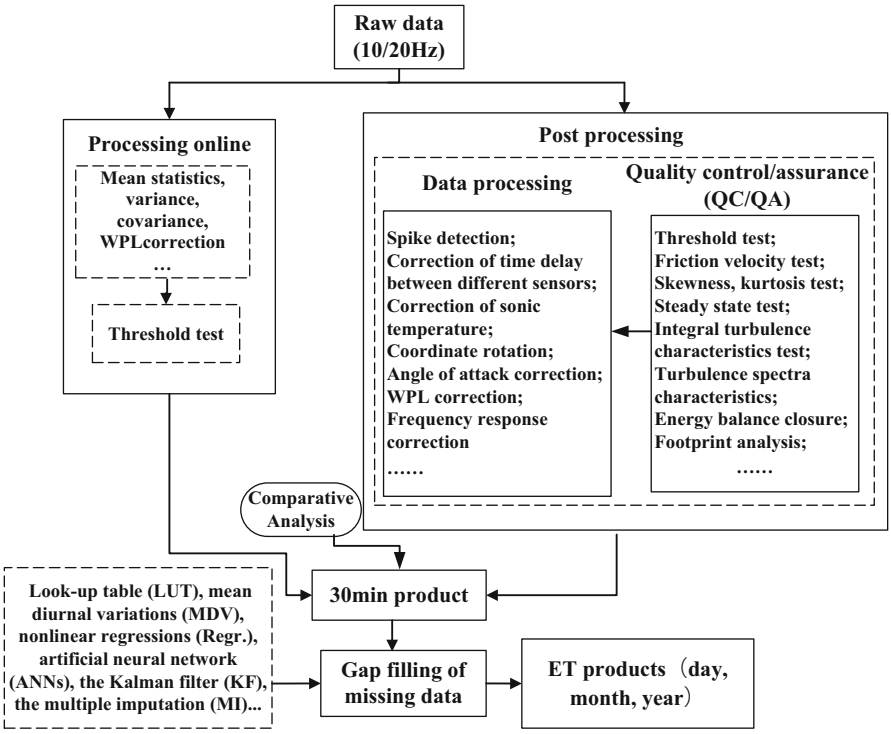

Fig. 4 EC data processing flowchart

There are a variety of software programs for flux calculations, including ECPack from Wageningen University, TK2/3 from the University of Bayreuth, EddySoft developed at the Max Planck Institute for Biogeochemistry in Jena, EdiRE software from the University of Edinburgh, and EddyPro software developed by LI-COR Company. The software programs include the necessary procedures, e.g., spike detection, sonic temperature correction, coordinate rotation, frequency response correction, WPL correction, quality control, and uncertainty assessment (in ECPack, TK3, EddyPro). The software programs can process EC raw data well and show common agreement (Mauder et al. 2008). Researchers can choose any suitable software to process EC data.

Footprint

Footprint analysis is now a recognized part of the establishment and placement of flux towers and the analysis of their output (Finnigan 2004). The turbulent fluxes obtained from EC measurements reflect the influence of the underlying surface on the turbulent exchange (Schmid 2002). It is necessary to determine the source area of the EC measurements using the footprint model before analyzing the characteristics of the surface fluxes. Generally, footprint models can be divided into two categories: numerical models, which emphasize simulation research and are complicated (Flesch et al. 1995), and analytical or semiempirical parameterized models, which emphasize applicability and are more concise (Horst and Weil 1992; Hsieh et al. 2000; Kormann and Meixner 2001).

The Eulerian analytic flux footprint model (Kormann and Meixner 2001) is commonly used to obtain the flux footprint of EC flux measurements, $f(x, y, z_m)$, as follows:

$$f(x, y, z_m) = D_y(x, y) f^y(x, z_m) \tag{12}$$

where x is the downwind distance pointing against the average horizontal wind direction, y is the crosswind wind distance, z_m is the measurement height, $f^y(x, z_m)$ is the crosswind integrated footprint, and $D_y(x, y)$ is the Gaussian crosswind distribution function of the lateral dispersion. The parameters of stability (Obukhov length), friction velocity, standard deviation of lateral wind speed, wind speed and direction, and measurement height are used as the input to the model.

In application, the most important issue for researchers is the source area. Generally, the source area is set to the P%, which is the fraction of the calculated footprint weight function with the most contribution to the total cumulative value within the horizontal source area. The equation can be expressed as:

$$P = \frac{\iint_{\Omega_P} f(x, y, z_m) dxdy}{\int_{-\infty}^{\infty} \int_{-\infty}^{\infty} f(x, y, z_m) dxdy} \tag{13}$$

EC systems are usually installed at a height of several meters with a source area generally covering several hundred meters. This concept is a robust tool to help

researchers to perform specific investigations, such as experimental design for flux measurements (Schmid 1997), analyzing the long-term ET variations (investigating specific surfaces, Liu et al. 2011, 2013), and validating remotely sensed ET at medium–high spatial resolution (choosing validated pixels, Jia et al. 2012; Bai et al. 2015).

Summary

The EC method has become increasingly common since the 1990s for measuring the water, heat, and carbon dioxide exchange between an ecosystem and the atmosphere. Some milestones in the development of the EC method can be found in Table 1.1 of Foken et al. (2012).

The advantages of the EC method include (1) direct measurement of the sensible heat, latent heat, CO_2, and momentum fluxes and other scalars, (2) continuous collection of fine temporal (e.g., 30 min, 1 h) and spatial (hundreds of meters) resolution data, and (3) automatic operation in the field. The disadvantages are (1) the requirement for careful data processing and corrections, (2) the requirement of a substantial source area, (3) the "unclosed" energy balance in the surface layer due to numerous reasons, and (4) the relatively large power consumption and requirement for regular calibration.

Scintillometer Method

A scintillometer is a device consisting of a transmitter and a receiver separated by a distance of several hundred meters to several kilometers that can measure the area-averaged sensible and latent heat fluxes based on Monin–Obukhov similarity theory (MOST). Scintillometers have now become common in hydrological and meteorological research (De Bruin 2009). As the measurement scale matches well with satellite pixels and model grids, this method has broad application prospects.

The transmitter of a scintillometer emits electromagnetic radiation that is scattered by the turbulent atmosphere, and the receiver detects and evaluates the intensity fluctuations of the transmitted signal. The magnitude of the fluctuations in the refractive index is usually measured in terms of the structure parameter C_n^2, which is the spectral amplitude of the refractive index fluctuations in the inertial subrange of turbulence (Wang et al. 1978). The structure parameter depends on the wavelength of radiation as a representation of the "turbulent strength" of the atmosphere. The National Oceanic and Atmospheric Administration (NOAA) scintillometer group first developed an instrument based on this method. Optical/near-infrared and microwave scintillometers have emerged since the 1980s and have been applied widely in field experiments since the mid-1990s (a commercial microwave scintillometer was developed in 2014 (RPG Radiometer Physics GmbH 2014) and applied worldwide since then). More detailed information about the history of scintillometry can be found in De Bruin and Wang (2017) and Ward (2017).

Theory

Optical/near-infrared scintillometers measure the sensible heat flux by relating the structure parameter to a temperature structure parameter and the Monin–Obukhov stability parameters. The microwave scintillometer (MWS) is sensitive to both the humidity and temperature structure parameters; however, the humidity structure parameter is the dominating influencing factor, which can be used to infer evapotranspiration. The combination of optical/near-infrared and microwave scintillometer (OMS), together with the related meteorological parameter and MOST, can be used to measure the area-averaged sensible and latent heat fluxes simultaneously.

The structure parameter of the refractive index of air, ${C_n}^2$ ($\mathrm{m}^{-2/3}$), is calculated from the variance of the natural logarithm of the intensity fluctuations (${\sigma_{\ln I}}^2$) using the following equations (Wang et al. 1978):

$$C_{n,LAS}^2 = 1.12\sigma_{\ln(I_{LAS})}^2 D^{7/3} L^{-3} \tag{14}$$

$$C_{n,MWS}^2 = 2.015\sigma_{\ln(I_{MWS})}^2 k^{-7/6} L^{-11/6} \tag{15}$$

where D is the aperture diameter (m), L is the path length (m), and k is the wave number. The refractive index of air is primarily affected by air temperature (T) and specific humidity (q) fluctuations, which are driven by sensible heat and latent heat fluxes. The index ${C_n}^2$ ($C_{n,\ LAS}^2$, $C_{n,\ MWS}^2$) is related to the temperature structure parameter, ${C_T}^2$ ($\mathrm{K}^2\ \mathrm{m}^{-2/3}$); the humidity structure parameter, ${C_q}^2$ ($\mathrm{kg}^2\ \mathrm{m}^{-6}\ \mathrm{m}^{-2/3}$); and a covariant term, C_{Tq} ($\mathrm{K\ kg\ m}^{-3}\ \mathrm{m}^{-2/3}$), and can be expressed as:

$$C_n^2, LAS = \frac{{A_{T,LAS}}^2}{\overline{T}^2} C_T^2 + 2\frac{A_{T,LAS}A_{q,LAS}}{\overline{T}\,\overline{q}} C_{Tq} + \frac{{A_{q,LAS}}^2}{\overline{q}^2} C_q^2 \tag{16}$$

$$C_n^2, MWS = \frac{{A_{T,MWS}}^2}{\overline{T}^2} C_T^2 + 2\frac{A_{T,MWS}A_{q,MWS}}{\overline{T}\,\overline{q}} C_{Tq} + \frac{{A_{q,MWS}}^2}{\overline{q}^2} C_q^2 \tag{17}$$

where the A-coefficients include the partial derivatives of the refractive index depending mainly on the temperature and humidity, which are obtained in related experiments. There are three variables (${C_T}^2$, ${C_q}^2$, C_{Tq}) in the two equations. Two methods can be used to solve for the variables:

1. Setting the parameter of R_{Tq}. Assume a correlation coefficient of temperature and humidity R_{Tq}, defining $C_{Tq} = R_{Tq}\sqrt{C_T^2 C_q^2}$ (Hill et al. 1988; Andreas 1989).
2. Bichromatic method based on near-infrared and MWS measurements (Lüdi et al. 2005).

After ${C_T}^2$, ${C_q}^2$, and C_{Tq} are obtained, the sensible heat and latent heat fluxes, H_{OMS} and LE_{OMS}, can be calculated according to MOST and the related meteorological parameters using the following equations:

$$\frac{C_T^2(z_{\mathrm{OMS}}-d)^{2/3}}{{T_*}^2}=f_T\left(\frac{z_{\mathrm{OMS}}-d}{L_{\mathrm{Ob}}}\right) \tag{18}$$

$$\frac{C_q^2(z_{\mathrm{OMS}}-d)^{2/3}}{{q_*}^2}=f_q\left(\frac{z_{\mathrm{OMS}}-d}{L_{\mathrm{Ob}}}\right) \tag{19}$$

$$H_{\mathrm{OMS}}=-\rho C_p u_* T_* \tag{20}$$

$$LE_{\mathrm{OMS}}=-\rho L_v u_* q_* \tag{21}$$

$$u_*=\frac{k_v u}{\ln\left(\frac{z-d}{z_{0m}}\right)-\Psi_m\left(\frac{z}{L_{\mathrm{Ob}}}\right)+\Psi_m\left(\frac{z_{0m}}{L_{\mathrm{Ob}}}\right)} \tag{22}$$

where z_{OMS} is the effective height of the scintillometer (m), d is the zero-plane displacement height (m), L_{Ob} is the Obukhov length (m) calculated via an iterative process, and f_T and f_q are the stability functions of temperature and specific humidity, respectively. There are several empirical functions under unstable (i.e., $L_{\mathrm{Ob}}<0$) and stable (i.e., $L_{\mathrm{Ob}}>0$) conditions (Andreas 1989; Thiermann and Grassl 1992; Hartogensis and De Bruin 2005). c_p is the specific heat capacity of air at a constant pressure (J kg^{-1} °C^{-1}), ρ is the density of air (kg m^{-3}), u_* is the friction velocity (m s^{-1}), T_* is the temperature scale (°C), q_* is the specific humidity scale (kg kg^{-1}), k_v is the von Kármán constant (0.40), u is the wind speed (m s^{-1}), z is the wind speed measurement height (m), z_{0m} is the aerodynamic roughness length (m), and Ψ_m is the stability correction function for the momentum transfer.

Installation and Maintenance

Scintillometers can be categorized as near-infrared (common wavelengths of 850 nm, 880 nm, and 940 nm) and microwave (common wavelengths of 1.86 mm, 3.19 mm, and 11.11 mm) according to the emission spectrum of the transmitter. The near-infrared range is widely used to measure the sensible heat flux, and the devices utilizing this range can be categorized as small-aperture scintillometer (SAS), large-aperture scintillometer (LAS), and extra-large-aperture scintillometer (XLAS) according to the aperture size. The main manufacturers are the Kipp & Zonen Company, Netherlands, and the Scintec Company, Germany. The MWS can measure latent heat flux directly, and the commercial manufacturer is Radiometer Physics GmbH (RPG) Company, Germany (Fig. 5).

The following section uses the most common near-infrared scintillometer (LAS) as an example to illustrate the installation and maintenance and also with some additional introductions to the MWS. The choice of observation site depends on the specific scientific issue of interest. After the observation site is selected, the LAS/MWS should be installed in the location that is least disturbed by the nearby ecosystem. The transmitter and receiver are usually placed in a north and south orientation to avoid direct sunlight at low solar elevation angles. LAS/MWS measurements are primarily effected by the center area of the path length. Therefore, the

Fig. 5 Scintillometer (LAS (BLS450, Scintec) and MWS; the picture on the *right* is from the RPG manual)

installation of the transmitter and receiver is fixed as firm as possible, and the influence of the platform is not considered. The platform can be a tripod, tower, building, mountain, etc., depending on the actual conditions. The path length of LAS/MWS should be perpendicular to the prevailing wind direction to ensure the largest source area of the observed fluxes. The automatic weather station can be installed in the center of the scintillometer's path length so that the meteorological elements (e.g., radiation, soil heat flux, air temperature and humidity, wind speed) represent the average conditions of the scintillometer's source area. Meanwhile, the height of the wind speed and air temperature sensors (used in the scintillometer calculation) should be the same as the effective height of the scintillometer. The effective height is an important parameter that is used to derive the sensible and latent heat fluxes. Both near-infrared and microwave scintillometer have their own weighting functions, and the OMS system also has a combined weighting function. The central area makes the greatest contribution to the near-infrared, microwave scintillometer and the OMS system. When the scintillometer system is operated at almost constant beam height over flat terrain, the installation height can be considered as the effective height. However, for slanted paths and over varying topographies, the effective height should be carefully calculated according to the atmosphere stability, topography, and weight function. The readers can refer to Hartogensis et al. (2003) for LAS and to Evans and De Bruin (2011) for the OMS system to obtain more information about the effective height. In field observations, the "saturation" phenomenon occurs in LAS measurements, especially when subjected to strong turbulence and scattering. To avoid this phenomenon, the relationship among the path length, effective height, and local sensible heat flux should be comprehensively considered. Usually, a longer path length is accompanied by a higher effective height when the sensible heat flux is constant; otherwise, a shorter path length corresponds to a lower effective height. Details can be found in the scintillometer manual.

The emission frequencies for the Boundary-Layer Scintillometer (BLS) series are 1 Hz, 5 Hz, 25 Hz, and 125 Hz, and those for the Kipp and Zonen LAS are 6.5–7.5 kHz. The emission frequency for MWS (RPG Company) is 160.8 GHz. The raw data for LAS is usually obtained during a 1-min collection (10-min or 30-

min post-processing period), and the data can be transferred to the researcher via wireless network (GPRS) in real time so that the data can be checked in a timely manner. The raw data for MWS are composed of several files, and the post-processed raw data for a 1-min or 10-min period can be transferred by GPRS. Routine scintillometer maintenance must also be performed regularly, i.e., at least monthly. Regular maintenance should include checking the signal, keeping the transmitter aligned to the receiver, and cleaning the mirror.

Data Processing and Quality Control

The determination of the sign of the heat flux is important. Previous near-infrared LAS measurements were unable to determine the sign and often used empirical methods (e.g., based on the sunrise and sunset, net radiation, or Obukhov length) (Lu et al. 2009). These methods are not required when using an OMS system. The co-spectrum provides the correlated structure parameter C_{Tq}, which can be used to calculate the correlation coefficient R_{Tq}:

$$R_{Tq} = \frac{C_{Tq}}{\sqrt{C_T^2 C_q^2}} \tag{23}$$

where R_{Tq} ranges between −1 and +1 and has the same sign as the $H \times LE$. The latent heat flux LE is almost always larger than 0, and even when it is less than 0, the absolute value is usually small. The OMS procedure assumes LE is always positive sign. In this case, R_{Tq} unambiguously provides the sign of the H.

Four steps are taken to ensure the quality of LAS data (Liu et al. 2013): (i) reject data for ${C_n}^2$ beyond the saturation criterion; (ii) reject data obtained during periods of precipitation; (iii) reject data when the demodulated signal is small; and (iv) reject data when the sensor is malfunctioning. The above procedures can also be used for MWS data.

The uncertainty of scintillometer measurements can be obtained by comparison with EC measurements on a relatively homogeneous surface. In general, good consistency is observed between scintillometer and EC measurements, with the sensible heat flux showing greater than 90% agreement (McAneney et al. 1995; Hoedjes et al. 2002; Kleissl et al. 2009; Xu et al. 2013). Scintillometer theory is based on MOST. To ascertain the scintillometer data quality (according to MOST), the observed values of $C_T^2 (z_{\mathrm{OMS}} - d)^{2/3} / {T_*}^2$ and $C_q^2 (z_{\mathrm{OMS}} - d)^{2/3} / {q_*}^2$ (${C_T}^2$ and ${C_q}^2$ from the scintillometer) can be plotted against the observed values of $(z_{\mathrm{OMS}} - d)/L$, together with the theoretical line from previous studies, such as Andreas (1989), Thiermann and Grassl (1992), and Hartogensis and De Bruin (2005). The values of T_*, q_*, and L can be taken from the EC measurements. The better consistency of observed values and theoretical line indicates the better of the scintillometer data quality.

During long-term observation, missing data will occur due to instrument malfunction, poor maintenance, bad weather conditions, and rejected bad data. Gap-filling methods, such as free convection, nonlinear regressions (regr.), dynamic linear regression (DLR), and harmonic analysis of times series (HANTS) (Bai et al. 2010), can be

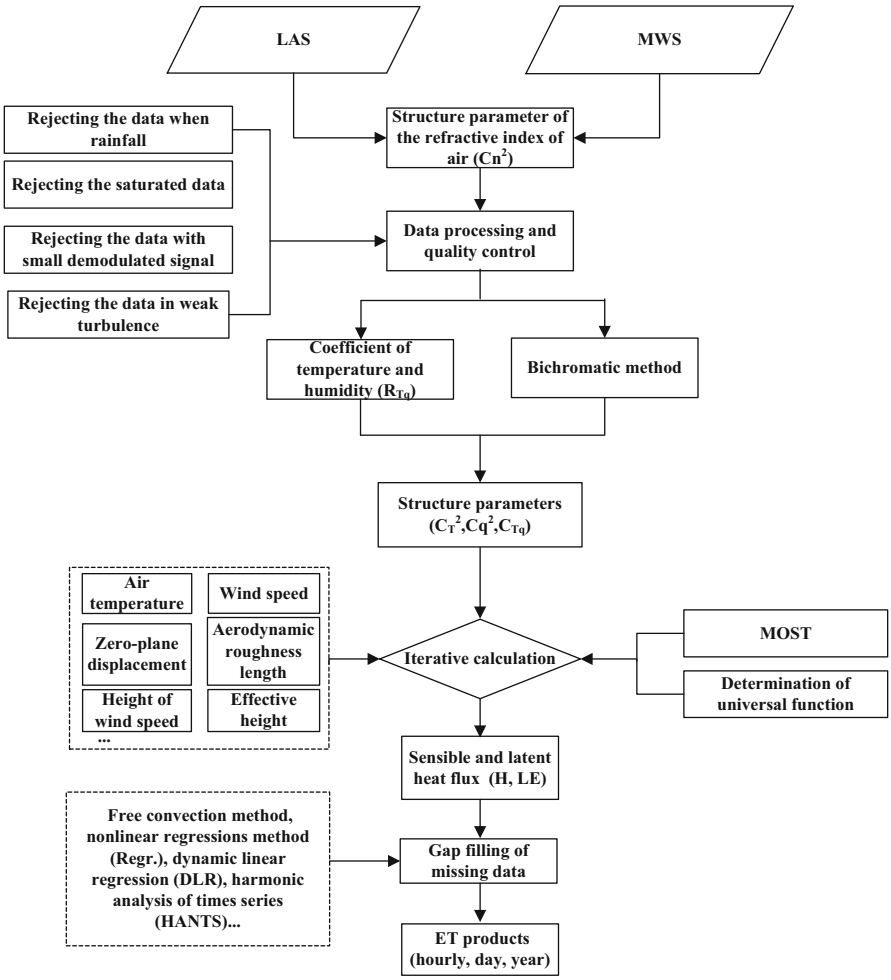

Fig. 6 Scintillometer data processing flowchart

applied to fill the gaps. The general scintillometer data processing flowchart is shown in Fig. 6.

Footprint

The equation for LAS flux observations can be obtained by combining the path-weighting function of the LAS (Meijninger et al. 2002) with the point flux footprint model (EC system):

$$f_{LAS}(x', y', z_m) = \int_{x_2}^{x_1} W(x) f(x - x', y - y', z_m) dx \tag{24}$$

where $W(x)$ is the path-weighting function of the LAS, x_1 and x_2 are the locations of the LAS transmitter and receiver, x and y denote points along the optical length of the LAS, and x' and y' are the coordinates upwind of each of the points (x and y).

The source area of LAS is usually on the scale of several kilometers, e.g., the LITFASS experiment in Germany (Meijninger et al. 2002) and the Heihe and Hai River Basin in China (Liu et al. 2011, 2013). These data can be applied to validate the ET at medium–low spatial resolution (Jia et al. 2012), for numerical model simulations (Xu et al. 2015), and for flux upscaling investigations (Liu et al. 2016). The source area of the OMS system uses similar equations that differ in the path-weighting function; however, it has not yet been reported in the literature.

Summary

Scintillometers can obtain the path-averaged surface fluxes of both sensible heat (near-infrared scintillometer) and latent heat (OMS system) and have the potential to bridge the gap between point observations and satellite pixel or model grid scales. Moreover, scintillometers are cheaper than the other instruments that are used to obtain area average fluxes, such as airborne EC and flux observation matrix. Additional advantages of scintillometers are that they can be used to acquire high temporal resolution averaged fluxes according to a specific objective and that they are relatively simple to operate and maintain in the field. Besides fluxes and structure parameters, scintillometers can also yield crosswind, rainfall, visibility, etc. (Ward 2017). Therefore, scintillometers have broad application prospects.

Nevertheless, scintillometers have several demerits. The primary disadvantage is that they depend on Monin–Obukhov similarity theory to calculate fluxes. Therefore, it must first be determined whether Monin–Obukhov similarity theory is applicable during data processing, especially in the stable boundary layer and roughness sublayer, as well as complex surfaces. The energy balance residual method, which requires the area-averaged net radiation and surface soil heat flux measurements, should be used to derive ET when using a near-infrared scintillometer. In the field observations, unsuitable meteorological conditions, such as precipitation, poor visibility, and weak turbulence, as well as tower vibrations and the power supply, restrict the application of scintillometers for long-term operation (Moene et al. 2009). In addition, the power consumption of MWS scintillometers is very large; it is better to use alternating current. The commercial MWS scintillometer has only recently been applied in field experiments; more research results should be summarized in the future.

Typical Evapotranspiration Observation Systems

A number of observation networks, observatories, or experiments have been carried out on various terrestrial surfaces throughout the world to determine ET.

ET Observation Network

The global network of FLUXNET was established in the mid-1990s; the first efforts of FLUXNET were to measure carbon, water, and energy fluxes on a quasi-continuous basis for a year or more. ET is one of the primary observation elements in various ecosystems with long-term observations, providing valuable datasets to study ET variations around the world (Wilson and Baldocchi 2000; Wever et al. 2002). The National Ecological Observatory Network (NEON), which is a continental-scale ecological observation facility founded in the USA, was completed in 2012 (Kuhlman et al. 2016). NEON has 81 field sites and will collect data for 30 years. These data can be applied to analyze long-term ET characteristics. At the catchment scale, ET is a major component in the water cycle, and it is the most challenging variable to measure at this scale due to the heterogeneity of the landscape. In the USA, the critical zone observatory (CZO) network was founded in 2007 (Anderson et al. 2008), including nine sub-CZOs. The function of CZO is to focus on the interconnected chemical, physical, and biological processes shaping Earth's surface at the catchment/watershed scale, including the overall watershed energy, carbon, and mass balance interactions. In Germany, the Terrestrial Environmental Observatories (TERENO) network, in which four typical terrestrial observatories were selected to monitor the land surface–atmosphere interactions, was established in 2008 (Bogena et al. 2006). The hydrological observatory (HOBE) was established in 2007 to investigate water resources using multi-instruments in the Skjern catchment in Denmark (Jensen and Illangasekare 2011). In China, a hydrometeorological observation network in the Heihe River Basin was established during the Watershed Allied Telemetry Experimental Research (WATER, 2008–2011) and completed in 2013 during the Heihe Watershed Allied Telemetry Experimental Research (HiWATER) projects (Li et al. 2009, 2013), which included three superstations and 18 ordinary stations to monitor the hydrological process in the Heihe watershed. In these typical watershed experiments, the ET measurements were essential or basic observations, and the primary observation techniques were micrometeorological methods, such as EC and LAS.

Global FLUXNET

In 1995, a network arose after discussions at the La Thuile workshop in Italy (Baldocchi et al. 1996). After the workshop, more flux sites and regional networks were established around the world. The flux measurement sites are linked across a confederation of regional networks in the USA, Europe, Canada, Oceania, Africa, Japan, Korea, and China, as well as other professional research organizations, in a global network, called FLUXNET. The FLUXNET project started circa 1997 with support from NASA and other organizations; it coordinates regional and global analyses of observations from micrometeorological tower sites. The flux tower sites mainly use the eddy covariance method to measure the exchanges of *ET*, *H*, and CO_2 between terrestrial ecosystems and the atmosphere.

The distribution of FLUXNET sites ranges from 70 °N to 30 °S, with underlying surfaces of boreal forest, tropical rainforest, evergreen broadleaf forest, deciduous broadleaf forest, evergreen needleleaf forest, deciduous needleleaf forest, mixed forest, woody savanna, savanna, temperate grassland, wetland, tundra, shrubland, cropland, barren, urban, etc. Till February 2017, the number of total registered sites in FLUXNET was 914, accounting for 7,479 site years (Fig. 7).

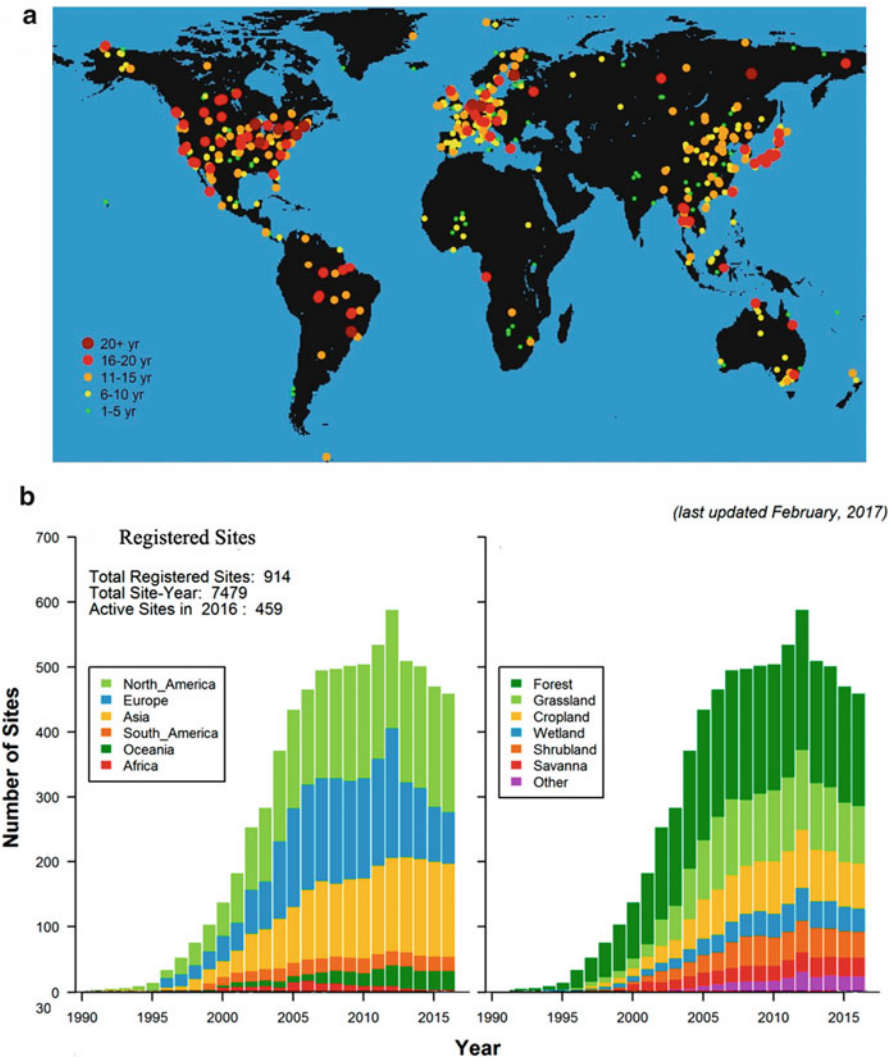

Fig. 7 (**a**) The spatial representativeness of the FLUXNET network and (**b**) summary of the tower sites that are registered in FLUXNET (data accessed in February 2017) (From http://fluxnet.fluxdata.org)

One of the main objectives of FLUXNET was to provide infrastructure to compile, archive, and distribute water, energy, and carbon flux measurements and meteorological data to the science community (Baldocchi et al. 2001). Several data synthesis activities have been conducted by the FLUXNET research community, and the most recently produced dataset is the FLUXNET2015 dataset (http://fluxnet.fluxdata.org/data/fluxnet2015-dataset/). Scientists around the world can use this dataset to conduct research. The dataset can be used to investigate the characteristics and controlling factors of ET (Wilson and Baldocchi 2000; Wever et al. 2002) and to validate and promote the development of evaporation at the regional and global scale by remote sensing estimations to better understand the water and energy cycles (Ershadi et al. 2014; Michel et al. 2016).

Watershed Observatories

The catchment scale has been adopted as the most appropriate scale for water legislation and management (Jensen and Illangasekare 2011). In this chapter, three watershed observatory systems in different countries, whose main objective was ET observations, were selected. In Germany, the TERENO project has established four observatories across Germany since 2008 (Bogena et al. 2006). In Denmark, a hydrological observatory, HOBE, was established in 2007 (Jensen and Illangasekare 2011). In China, the hydrometeorological observation network was established in 2008 during WATER and was completed in 2013 during the HiWATER projects (Li et al. 2009, 2013).

TERENO

In 2008, the Terrestrial Environmental Observatories (TERENO) network was established in Germany as an interdisciplinary research program to observe and explore the long-term ecological, social, and economic impacts of global change at the regional level (Zacharias et al. 2011). Within TERENO, four terrestrial observatories were selected as representing the highest vulnerability with respect to climate change effects in Germany (Fig. 8).

The observation instruments included EC, automatic weather station, isotope, sap flow (thermal dissipation probe, TDP), lysimeter, etc. The TERENO observations used 126 lysimeters at 12 different test sites and one or two EC sets in each catchment to monitor ET.

In addition, there were installed 150 wireless soil temperature/moisture networks in the Wüstebach catchment, as well as runoff, groundwater, and water quality measurements. Additionally, there were cosmic-ray sets in the Wüstebach (one set), Schäfertal (one set), and Rur (ten sets) catchments and 245 rain gauges in the Bode catchment. Furthermore, airborne experiments were also conducted in TERENO, and the airborne sensors included hyperspectral, infrared, microwave radiometer, and lidar. TERENO is a large-scale project, with an Earth observation network across Germany that extends from the North German lowlands to the Bavarian Alps. The observed data and additional information can be found on the website (http://teodoor.icg.kfa-juelich.de/overview-en).

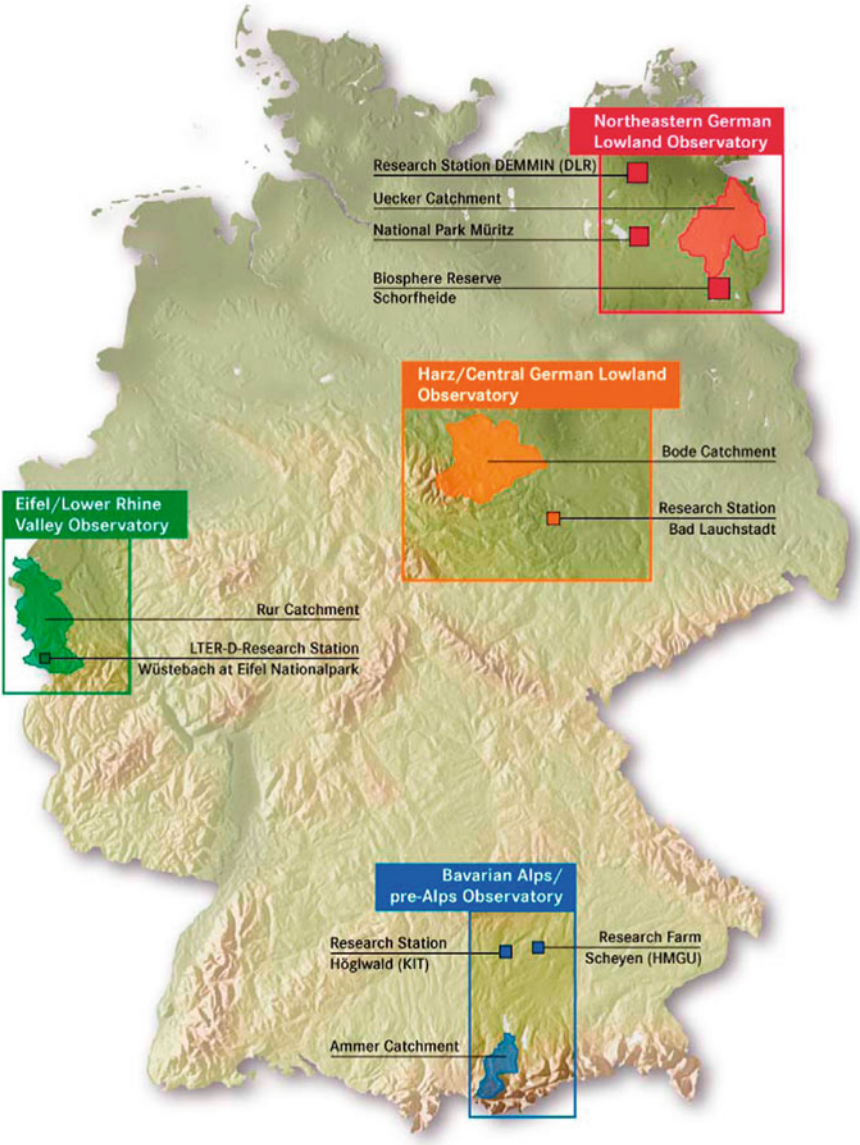

Fig. 8 TERENO observatories in Germany (From Zacharias et al. 2011)

HOBE

HOBE, a hydrological observatory, was established in 2007 in the Skjern catchment located in the western part of Denmark. The entire catchment covers 2,500 km^2 of mostly rural with land cover including grain, corn, grass, forest, heath, and urban (Fig. 9). The overall objectives of the research are to establish a hydrological

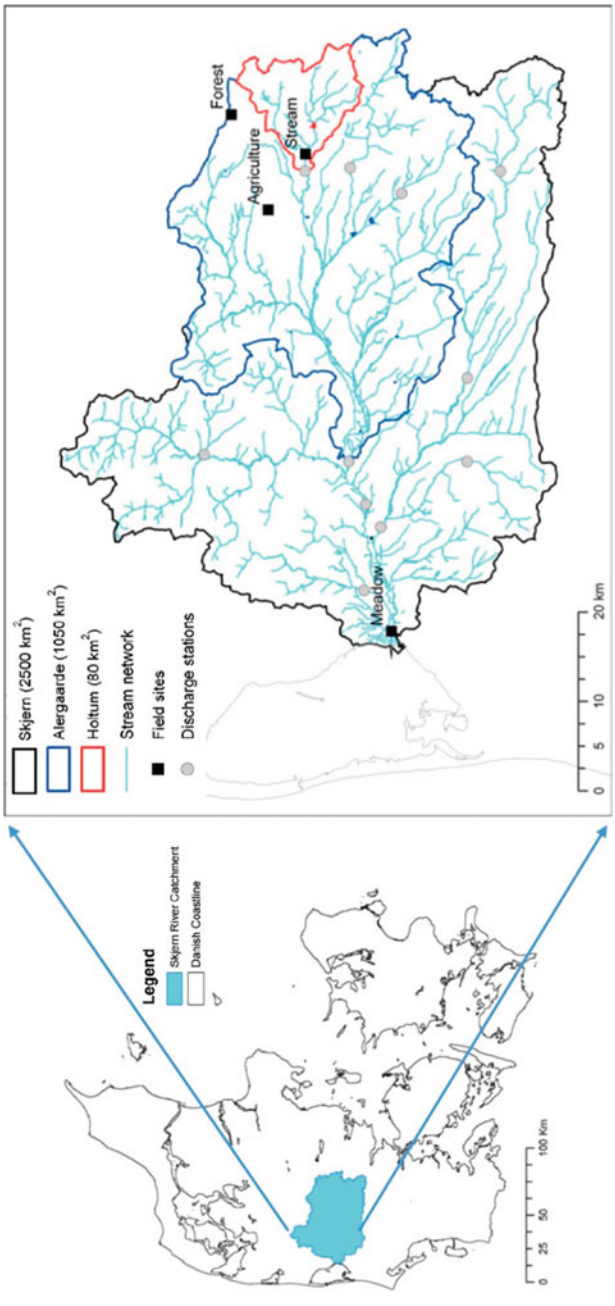

Fig. 9 Location of the Skjern River catchment in Western Denmark (From Jensen and Illangasekare 2011). The forest site, agricultural site, and meadow site were installed the eddy covariance systems

observation platform with an interdisciplinary focus and to better understand the water resources and reduce the uncertainty in the water balance closure at the catchment scale.

The observation instruments included three eddy covariance systems and automatic weather stations, 30 soil moisture and temperature wireless networks, three cosmic-ray measurement sites and isotope, etc. In addition, airborne campaigns (passive L-band microwave radiometer) were conducted to calibrate/validate the SMOS products.

Three eddy covariance flux stations were established to obtain the evapotranspiration and energy balance (agricultural land, spruce plantation, and wet grassland), representing the main land-use types of the catchment (Fig. 9). Measurements have been ongoing since 2008, and these measurements provide a continuous flux dataset for ET analysis and for modeling and scaling of ET to the entire catchment (Ringgaard et al. 2011). More information, including the data, can be found on the website (http://www.hobecenter.dk/).

Heihe Hydrometeorological Observatory

The Heihe River Basin (HRB) is a typical inland river basin, the second largest in China. The HRB is an area of approximately 143,000 km^2, covering Qilian County in Qinghai Province (upstream), Zhangye City in Gansu Province (midstream), and Ejin Banner in Inner Mongolia (downstream). The land cover is characterized by distinct cold and arid landscapes, glaciers, frozen soil, alpine meadow, forest, irrigated crops, riparian ecosystem, and desert, which are distributed from upstream to downstream (Li et al. 2013).

During the WATER experiment from 2008 to 2011 (Li et al. 2009), a prototype of a hydrometeorology observatory was established, in which three long-term EC systems (A'rou site, grassland; Yingke site, cropland; Guantan site, forest) were established in the upstream and midstream areas, in addition to one group of large-aperture scintillometer and three automatic weather stations (AWSs). The HiWATER project was launched in 2012 as a comprehensive eco-hydrological experiment in the framework of the Heihe Plan, based on the diverse needs of the interdisciplinary studies of the research plan and the existing observation infrastructure in the basin (Li et al. 2013). The overall objectives of HiWATER are to improve the observability of hydrological and ecological processes, to build a world-class watershed observation system, and to enhance the applicability of remote sensing in integrated eco-hydrological studies and water recourse management at the basin scale.

Through the HiWATER project, a comprehensive hydrometeorological observatory was established in 2013. The network covers the upstream, midstream, and downstream zones, including three superstations and 18 ordinary stations, covering the main underlying surfaces in the basin, including alpine meadow, cropland, desert, wetland, frozen soil, *Tamarix chinensis*, and *Populus euphratica*. The superstation is a multi-scale observation system for ET measurements, consisting of an LAS, EC, lysimeter, TDP, and meteorological element gradient observation system (seven layers of wind speed/direction and air temperature/humidity, precipitation, air pressure, infrared temperature, four-component radiation, photosynthetically active

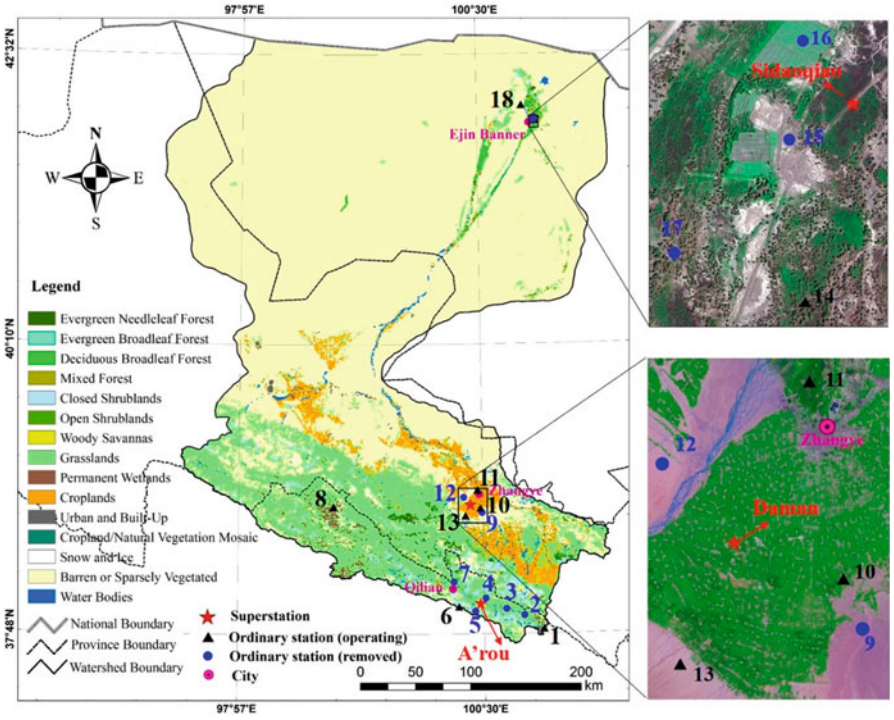

Fig. 10 The hydrometeorological observatory over the Heihe River Basin (*red star*, superstations; *black triangle*, ordinary stations in operation; *blue circles*, ordinary stations have been removed. Numbers *1–8* are stations of Jingyangling, E'Bao, Huangcaogou, A'rou sunny slope, A'rou shady slope, Yakou, Huangzangsi, and Dashalong, respectively, in upstream; *9–13* are stations of Shenshawo sandy desert, Heihe remote sensing, Zhangye wetland, Bajitan Gobi, and Huazhaizi desert steppe, respectively, in midstream; *14–18* are stations of mixed forest, barren land, cropland, *Populus* forest, and desert station, respectively, in downstream)

radiation, soil heat flux, soil temperature/moisture profile, etc.), as well as a cosmic ray, and a wireless soil temperature and moisture network. The ordinary stations comprise an EC and an AWS. In 2016, there were three superstations and eight ordinary stations (the other ten ordinary stations were removed, *blue circles* in Fig. 10) in operation after comprehensive consideration (Fig. 10).

Additionally, airborne remote sensing experiments were conducted during the HiWATER project. The airborne experiments in the upstream and midstream areas were conducted during June 29–August 29, 2012, which included an imaging spectrometer, multi-angle thermal infrared camera (CASI, TASI, WiDAS), light detection and ranging (lidar), microwave radiometer (PLMR), etc. The downstream airborne experiment was conducted from July 29 to August 4, 2014, which included lidar, hyperspectral imager, thermal imager, etc. Airborne lidar and a charge-coupled device (CCD) were also used in the upstream airborne experiments on October 1 and 2, 2014 (Li et al. 2013). The corresponding satellite remote sensing data products

were produced, including the ET, fractional snow cover area, surface temperature/emissivity, soil moisture, leaf area index (LAI), fractional vegetation cover (FVC), compositing vegetation index (NDVI/EVI), fraction of absorbed photosynthetically active radiation (FPAR), crop phenology, net primary productivity (NPP), digital elevation model (DEM), land cover/use, etc. All the data were carefully processed, subjected to quality control, and released online at http://www.heihedata.org/hiwater (Chinese version) and http://card.westgis.ac.cn/hiwater (English version).

ET Observation Experiments

Several large land surface process experiments have been implemented worldwide, e.g., the First ISLSCP Field Experiment (FIFE, America; Sellers et al. 1988), the Hydrologic Atmospheric Pilot Experiment–Modélisation duBilan Hydrique (HAPEX-MOBILHY, France; André et al. 1986), the Hydrologic Atmospheric Pilot Experiment in the Sahel (HAPEX-Sahel, Niger; Goutorbe et al. 1994), the Northern Hemisphere Climate Processes Land Surface Experiment (NOPEX, Sweden; Halldin et al. 1999), the Boreal Ecosystem-Atmosphere Study (BOREAS, Canada; Sellers et al. 1995), Lindenberg Inhomogeneous Terrain-Fluxes Between Atmosphere and Surface: A Long-Term Study (LITFASS-98, LITFASS-2003, LITFASS-2009, Germany; Beyrich et al. 2002, 2012; Beyrich and Mengelkamp 2006), and the Multi-Scale Observation Experiment on Evapotranspiration over Heterogeneous Land Surfaces 2012 in the Heihe Watershed Allied Telemetry Experimental Research (HiWATER-MUSOEXE, China, Liu et al. 2016). In these experiments, the primary objective was to measure the interactions of the energy and water fluxes (especially ET) between the surface and the atmosphere. In the following section, several of these experiments are presented in greater detail.

LITFASS Experiment

LITFASS, an acronym for "Lindenberg Inhomogeneous Terrain-Fluxes Between Atmosphere and Surface: A Long-Term Study," was launched in 1995 near the Meteorological Observatory Lindenberg (MOL) in Northeast Germany. The objective of the project was to contribute to solving the problem of the area-averaging of fluxes over a heterogeneous landscape based on coupling between measurements and modeling activities and to develop a strategy for the operational determination of the area-averaged turbulence fluxes of heat, momentum, and water vapor over a heterogeneous landscape (Beyrich et al. 2002). LITFASS-98 and LITFASS-2003 are taken as examples to introduce the LITFASS experiment.

The initial field campaign, LITFASS-98, was conducted in May and June 1998 and was designed to focus on the experimental investigation of the atmospheric boundary-layer structure and the exchange of momentum, heat, and water vapor over a heterogeneous land surface (Beyrich et al. 2002). The study region covers a 20×20 km^2 area with land-use types of forest and agricultural fields, lakes, villages, and traffic roads (Fig. 11).

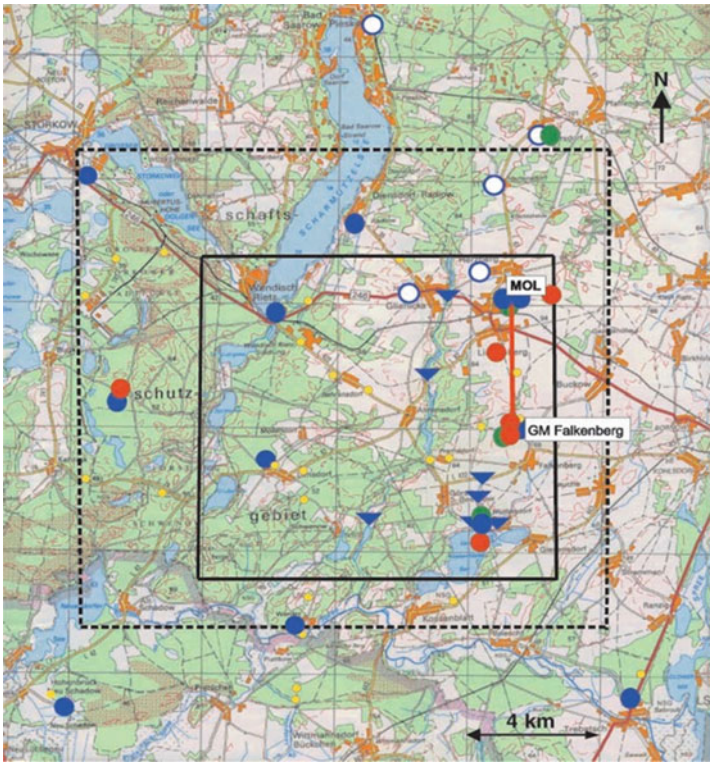

Fig. 11 The LITFASS area and the experimental setup during the LITFASS-98 experiment (From Beyrich et al. 2002) (*Bright areas mark* agricultural farmland, *green areas mark* forest, *blue areas* are lakes. The symbols are as follows: *red circles*, micrometeorological stations; *filled blue circles*, recording rain gauges; *open blue circles*, Hellmann-type rain gauges; *blue triangles*, water table gauges; *green circles*, infrared radiometers; *yellow points*, monitoring sites; *red line*, scintillometer path; *solid/dashed black boxes*, Helipod = Do128 flight pattern)

Micrometeorological and turbulence measurements (using an EC system) were conducted at five sites to characterize the interactions between the atmosphere and different types of underlying surfaces (grass, barley, triticale, forest, water). An LAS was operated at a distance of 4.7 km and a height of 45 m, covering a surface primarily composed of forest, grass and water. A special flux instrumentation intercomparison was performed after the main field phase of the LITFASS-98 experiment. Simultaneous flight measurements (fast temperature and humidity, airborne EC) were performed on June 18, 1998, using two research aircraft systems. Additionally, airborne lidar observations were conducted on June 3, 8, 13, and 18, 1998.

LITFASS-2003 was performed the same region in May and June 2003 (Beyrich and Mengelkamp 2006). The LITFASS measurement facilities were located at the MOL, including a boundary-layer field site (99 m meteorological tower, a sodar/

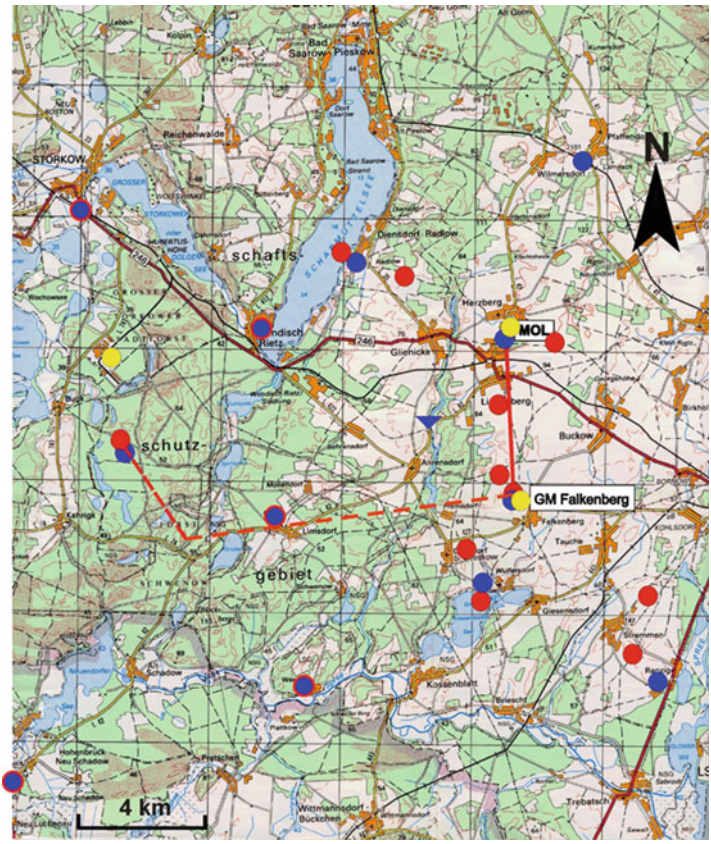

Fig. 12 The experimental setup and measuring strategy of the LITFASS-2003 experiment (From Beyrich and Mengelkamp 2006). *Red circle*, micrometeorological station; *yellow circle*, remote sensing site; *blue circle*, rain gauge; *blue circle with red ring*, rain gauge with global radiation sensor; *blue triangle*, water table measurement; *red solid/dashed line*, long-distance scintillometer path

RASS), a network of micrometeorological (flux) stations over different land-use classes, networks of automatically recording rain gauges and global radiation sensors, and a large-aperture scintillometer. The facility has been in continuous operation since summer 2001. More systems and instruments were added for the LITFASS-2003 experiment, including 14 micrometeorological and flux stations, laser scintillometers at five sites, three LAS systems, and an MWS. The 14 EC sets were composed of a flux observation matrix, including one set each in barley, triticale, and forest; two sets each in grass, maize, rye, and water; and three sets each in rape. The three LAS systems were operated over distances of 3–10 km to determine the area-averaged sensible heat flux, and an MWS was placed along one of the LAS paths over a distance of 4.7 km to determine the latent heat flux. Moreover, a Helipod hanging a turbulence probe recorded more than 60 flight hours (airborne EC) during May 23–June 17, 2013 (Fig. 12).

The LITFASS experiment provided a comprehensive and unique dataset on land surface-atmosphere interactions over a heterogeneous land surface. The turbulence intercomparison was performed in the experiment, and a complete quality-controlled time series of surface fluxes was created (Beyrich et al. 2002; Beyrich and Mengelkamp 2006).

HiWATER-MUSOEXE Experiment

In the HiWATER experiment, HiWATER-MUSOEXE in Zhangye City of Gansu Province, located in the middle reaches of the HRB, was established between May 3 and September 21, 2012, as the first thematic experiment: the Multi-Scale Observation Experiment on Evapotranspiration over Heterogeneous Land Surfaces (HiWATER-MUSOEXE). The objectives were to capture the 3-D dynamic characteristics of water and heat interactions between the surface and the atmosphere to better understand the ET process under the heterogeneous surface, to reveal the spatial heterogeneity of ET and its influence mechanism, to develop the upscaling methods for ET, and to provide ground truth values at the satellite pixel scale to develop and validate the ET remote sensing estimation model.

HiWATER-MUSOEXE was composed of two nested matrices: one large experimental area (30 km × 30 km) and one kernel experimental area (5.5 km × 5.5 km) (Liu et al. 2016). The large experimental area contained one superstation (within the oasis, cropland) and four ordinary stations (around the oasis), with underlying desert, desert steppe, Gobi, and wetland surfaces. The primary objectives were focused on studying the temporal–spatial variation of evapotranspiration (ET) and the effects of advection in the oasis-desert ecosystem. The kernel experimental area was located in the Yingke and Daman irrigation district, and the main surfaces were maize, residential area, vegetable, and orchard. These areas were separated into rows and columns by shelterbelts. Together, they represent the land cover and planting structure in the oasis of the middle reaches of the HRB. The heterogeneity of ET and the ET acquisition at the pixel scale were investigated in the kernel experimental area. Moreover, 17 elementary sampling plots were divided according to the distribution of crops, shelterbelts, residential areas, roads, and canals, as well as according to soil moisture and irrigation status. These divisions resulted in one residential area site, one orchard site, one vegetable site, and 14 maize sites. In each plot, one EC and one AWS were installed to observe the sensible heat flux, latent heat flux, and meteorological elements. Two EC sets and seven layers of meteorological gradient observation systems were installed at the Daman superstation. Moreover, the transpiration of shelterbelts with different heights and diameters at breast height (DBH) was measured using a TDP at three sites, representing the mean conditions of the shelter-forest in the study area. Three TDP probes were installed at a height of 1.3 m on three poplar trees at each site. Additionally, four groups of near-infrared LASs (eight sets with two sets in each group) were installed in the 3 × 3 and 2 × 1 MODIS pixels within the kernel experimental area (three groups in three 3 × 1 MODIS pixels, named LAS1 to LAS3 from west to east and one group in one 2 × 1 MODIS pixel, LAS4). In each LAS group, we primarily used the BLS series scintillometer data and only used the data measured by another scintillometer (zzLAS developed

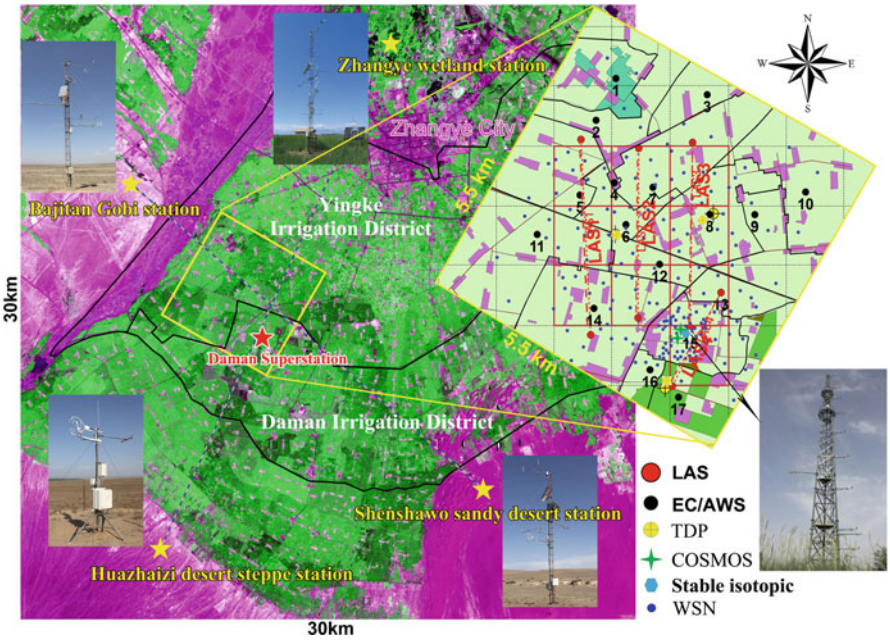

Fig. 13 Multi-Scale Observation Experiment on Evapotranspiration over Heterogeneous Land Surfaces (HiWATER-MUSOEXE)

by this chapter author's group or Kipp and Zonen LAS) if the BLS scintillometer measurements were missing. In addition, two cosmic-ray observations and a stable isotopic observation were conducted around the Daman superstation. There were also 180 wireless soil temperature and moisture network (WSN, 4 cm, 10 cm, 20 cm, and 40 cm) (Jin et al. 2014) and 50 leaf area index networks (LAInets) in the kernel experiment area (Qu et al. 2014) (Fig. 13).

Overall, 22 EC system sets, eight LAS sets, 21 AWS sets, two cosmic-ray sets, three group TDP sets, a stable isotopic observation, 180 WSNs, and 50 LAInets were included in the flux observation matrix. Additionally, the auxiliary parameters of ground-based observations were also measured, including GPS sounding and aerosol, spectral reflectance, emissivity, FVC, LAI/FPAR, photosynthesis, vegetation chlorophyll content, biomass, plant height, soil respiration, soil parameters, irrigation and field management information, etc.

Airborne remote sensing observations were also performed using imaging spectrometers (i.e., CASI and TASI system), a multi-angle thermal infrared camera (WiDAS), lidar, a CCD camera, and a microwave radiometer (L bands) during flight from June 29 to the end of August 2012. Satellite remote sensing data, including ASTER, Landsat ETM+, COSMO-SkyMed, SPOT, TerraSAR-X, WorldView, PROBA CHRIS, QuickBird, ZIYUAN-3 (ZY-3), and Radarsat-2, were also

collected during HiWATER-MUSOEXE. The corresponding satellite remote sensing data products were produced, including ET, surface temperature/emissivity, LAI, FVC, NDVI/EVI, FPAR, crop phenology, and land cover/use. All the datasets were carefully screened and processed, and the dataset were released online at http://www.heihedata.org/hiwater (Chinese version) and http://card.westgis.ac.cn/hiwater (English version).

To evaluate the differences among these flux instruments, a comparison of the surface energy flux measurement systems was conducted during May 14–24, 2012, prior to HiWATER-MUSOEXE. The comparison field was located in the Bajitan Gobi desert (a nearly flat and open surface), west of Zhangye City. In total, 20 EC sets, seven LAS sets, and 18 radiometer sets from HiWATER-MUSOEXE were included in the comparison (Xu et al. 2013). The comparison results were used to assess the consistency and reliability of instruments used in HiWATER-MUSOEXE, to guide the layout and installation of instruments, and to aid the subsequent data processing and analysis.

Conclusions and Outlook

ET is affected by multiple factors, e.g., meteorological factors, vegetation factors, and soil water content, and it is difficult to measure accurately. Among the ET observation methods, micrometeorological methods are the most commonly used due to the high temporal resolution, large spatial observation scale, and relatively high accuracy. In this chapter, the typical meteorological methods measuring ET were presented, including the Bowen ratio-energy balance method, eddy covariance method, and scintillometer method. The development of each method was briefly introduced. Afterward, the theory, installation and maintenance, data processing and quality control, and footprint were expounded, and a short summary of the advantages and disadvantages of each method was presented. Additionally, ET measurements at observational networks and intensive experiments were introduced.

The observational theory, temporal–spatial scale, and precision of each ET measurement method are different. In field experiments, researchers can select a suitable method according to their study objectives. Observational site selection, installation and maintenance of the instrument, data processing, and quality control are the key factors and core contents of ET observations.

Ground ET measurements are usually considered as the ground truth to calibrate and validate remotely sensed ET products or results simulated via land surface models, hydrologic models, or ecological models. However, the observation source area of micrometeorological methods typically has a length of hundreds to thousands of meters, and the source area is affected by the measurement height, wind speed and direction, atmospheric stability, and surface roughness length. Therefore, the source area of flux measurements does not always fully cover one or several satellite pixels, resulting in the problem of scale mismatch between the ground measurements and the remotely sensed estimations. In the future, large-scale ET observational methods

should be developed and improved, such as OMSs and airborne EC, which can directly obtain large-scale ground ET measurements. Additionally, flux observation matrices should be constructed to upscale multi-site ET to the satellite pixel scale or model grid scale using various upscaling methods.

References

N. Alavi, J.S. Warland, A.A. Berg, Filling gaps in evapotranspiration measurements for water budget studies: evaluation of a Kalman filtering approach. Agric. For. Meteorol. **141**, 57–66 (2006)

R.G. Allen, L.S. Pereira, T.A. Howell, M.E. Jensen, Evapotranspiration information reporting: I. Factors governing measurement accuracy. Agric. Water Manag. **98**, 899–920 (2011)

S.P. Anderson, R.C. Bales, C.J. Duffy, Critical zone observatories: building a network to advance interdisciplinary study of earth surface processes. Mineral. Mag. **72**(1), 7–10 (2008)

J.C. André, J.P. Goutorbe, A. Perrier, HAPEX–MOBLIHY: a hydrologic atmospheric experiment for the study of water budget and evaporation flux at the climatic scale. Bull. Am. Meteorol. Soc. **67**(2), 138–144 (1986)

E.L. Andreas, Two-wavelength method of measuring path-averaged turbulent surface heat fluxes. J. Atmos. Ocean. Technol. **62**, 280–292 (1989)

J. Bai, S.M. Liu, X.P. Ding, L. Lu, A study of the processing method of large aperture scintillometer observation data. Adv. Earth Science **25**(11), 1148–1165 (2010.) (In Chinese with English abstract)

J. Bai, L. Jia, S.M. Liu, Z.W. Xu, G.C. Hu, M.J. Zhu, Characterizing the footprint of eddy covariance system and large aperture scintillometer measurements to validate satellite-based surface fluxes. IEEE Geosci. Remote Sens. Lett. **12**(5), 943–947 (2015)

D. Baldocchi, R. Valentini, S. Running, W. Oechel, R. Dahlman, Strategies f or measuring and modelling carbon dioxide and water vapour fluxes over terrestrial ecosystems. Glob. Chang. Biol. **2**, 159–168 (1996)

D. Baldocchi, E. Falge, L.H. Gu, R. Olson, D. Hollinger, S. Running, P. Anthoni, C. Bernhofer, K. Davis, R. Evans, J. Fuentes, A. Goldstein, G. Katul, B. Law, X.H. Lee, Y. Malhi, T. Meyers, W. Munger, W. Oechel, K.T. Paw U, K. Pilegaard, H.P. Schmid, R. Valentini, S. Verma, T. Vesala, K. Wilson, S. Wofsy, FLUXNET: a net tool to study the temporal and spatial variability of ecosystem-scale carbon dioxide, water vapor, and energy flux densities. Bull. Am. Meteorol. Soc. **82**(11), 2415–2434 (2001)

F. Beyrich, H. Mengelkamp, Evaporation over a heterogeneous land surface: EVA_GRIPS and the LITFASS-2003 experiment – an overview. Bound.-Layer Meteorol. **121**, 5–32 (2006)

F. Beyrich, H.J. Herzog, J. Neisser, The LIFASS project of DWD and the LITFASS-98 experiment: the project strategy and the experimental setup. Theor. Appl. Climatol. **73**, 3–18 (2002)

F. Beyrich, J. Bange, O.K. Hartogensis, S. Raasch, M. Braam, D. van Dinther, D. Gräf, B. van Kesteren, A.C. van den Kroonenberg, B. Maronga, S. Martin, A.F. Moene, Towards a validation of scintillometer measurements: the LITFASS-2009 experiment. Bound.-Layer Meteorol. **144**, 83–112 (2012)

H. Bogena, K. Schulz, H. Vereeken, Towards a network of observatories in terrestrial environmental research. Adv. Geosci. **9**, 109–114 (2006)

I.S. Bowen, The ratio of heat losses by conduction and by evaporation from any water surface. Phys. Rev. **27**(6), 779–787 (1926)

P. Cellier, Y. Brunet, Flux–gradient relationships above tall plant canopies. Agric. For. Meteorol. **58**, 93–117 (1992)

P. Cellier, A. Olioso, A simple system for automated long term Bowen ratio measurement. Agric. For. Meteorol. **66**, 81–92 (1993)

D. Charuchittipan, W. Babel, M. Mauder, J.P. Leps, T. Foken, Extension of the averaging time in eddy-covariance measurements and its effect on the energy balance closure. Bound.-Layer Meteorol. **152**(3), 303–327 (2014)

J.D. Cooper, Water use of a tea estate from soil moisture measurements. East Afr. Agric. For. J. **43**, 102–121 (1979)

H.A.R. De Bruin, Time to think, reflections of a pre-pensioned scintillometer researcher. Bull. Am. Meteorol. Soc. **90**, ES17–ES26 (2009)

H.A.R. De Bruin, J.M. Wang, Scintillometry: a review. ResearchGate (2017). https://www.researchgate.net/pulications/316285424

D. Dragoni, A.N. Lakso, R.M. Piccioni, Transpiration of apple trees in a humid climate using heat pulse sap flow gauges calibrated with whole-canopy gas exchange chambers. Agric. For. Meteorol. **130**, 85–94 (2005)

A. Ershadi, M.F. McCabe, J.P. Evans, N.W. Chaney, E.F. Wood, Multi-site evaluation of terrestrial evaporation models using FLUXNET data. Agric. For. Meteorol. **187**, 46–61 (2014)

J. Evans, H.A.R. De Bruin, The effective height of a two-wavelength scintillometer system. Bound.-Layer Meteorol. **141**(1), 165–177 (2011)

E. Falge, D.D. Baldocchi, R. Olson, P. Anthoni, M. Aubinet, C. Bernhofer, G. Burba, R. Ceulemans, R. Clement, H. Dolman, A. Granier, P. Gross, T. Grünwald, D. Hollinger, N.O. Jensen, G. Katul, P. Keronen, A. Kowalski, C.T. Lai, B.E. Law, T. Meyers, J. Moncrieff, E. Moors, J.W. Munger, K. Pilegaard, ü. Rannik, A. Rebmann, C. Suyker, J. Tenhunen, K. Tu, S. Verma, T. Vesala, K. Wilson, S. Wofsy, Gap filling strategies for defensible annual sums of net ecosystem exchange. Agric. For. Meteorol. **107**, 43–69 (2001)

C. Feigenwinter, C. Bernhofer, R. Vogt, The influence of advection on the short term CO_2-budget in an above a forest canopy. Bound.-Layer Meteorol. **113**, 201–224 (2004)

P.L. Finkelstein, P.F. Sims, Sampling error in eddy correlation flux measurements. J. Geophys. Res. **106**(D4), 3503–3509 (2001)

J. Finnigan, The footprint concept in complex terrain. Agric. For. Meteorol. **127**, 117–129 (2004)

T.K. Flesch, J.D. Wilson, E. Yee, Backward-time Lagrangian stochastic dispersion models and their application to estimate gaseous emissions. J. Appl. Meteorol. **34**(6), 1320–1332 (1995)

T. Foken, The energy balance closure problem: an overview. Ecol. Appl. **18**(6), 1351–1367 (2008)

T. Foken, S.P. Oncley, Results of the workshop Instrumental and methodical problems of land surface flux measurements. Bull. Am. Meteorol. Soc. **76**, 1191–1193 (1995)

T. Foken, B. Wichura, Tools for quality assessment of surface-based flux measurements. Agric. For. Meteorol. **78**, 83–105 (1996)

T. Foken, M. Göckede, M. Mauder, L. Mahrt, B. Amiro, W. Munger, Post-field data quality control, in *Handbook of Micrometeorology*, ed. by X. Lee et al. (Kluwer, Dordrecht, 2004), pp. 181–208

T. Foken, M. Mauder, C. Liebethal, F. Wimmer, F. Beyrich, J.P. Leps, S. Raasch, H.A.R. De Bruin, W.M.L. Meijninger, J. Bange, Energy balance closure for the LITFASS-2003 experiment. Theor. Appl. Climatol. **101**, 149–160 (2010)

T. Foken, M. Aubinet, R. Leuning, The eddy covariance method, in Eddy Covariance: A Practical Guide to Measurement and Data Analysis, Springer Atmospheric Sciences, ed. by M. Aubinet et al. (Springer, Dordrecht, 2012). https://doi.org/10.1007/978-94-007-2351-1_1

L.J. Fritschen, C.L. Fritschen, Bowen ratio energy balance method, in *Micrometeorology in Agricultural Systems*, ed. by J.L. Hatfield, J.M. Baker. Agronomy Series, vol. 47 (American Society of Agronomy, Madison, 2005), pp. 397–405

L.J. Fritschen, J.R. Simpson, Surface energy balance and radiation systems: general description and improvements. J. Appl. Meteorol. **28**, 680–689 (1989)

L.J. Fritschen, L.W. Gay, J.R. Simpson, The effect of a moisture step change and advective conditions on the energy balance components of irrigated alfalfa, in *Proceedings of the 16th Conference on Agricultural and Forest Meteorology*, American Meteorological Society, Boston, 21–24 May 1983, pp. 83–86

W.U. Garstka, Design of the automatic recording in-place lysimeters near Coshocton, Ohio. Soil Sci. Soc. Am. Proc. **2**, 555–559 (1937)

J.P. Goutorbe, T. Lebel, A. Tinga, P. Bessemoulin, J. Brouwer, A.J. Dolman, E.T. Engman, J.H.C. Gash, M. Hoepffner, P. Kabat, Y.H. Kerr, B. Monteny, S. Prince, F. Said, P. Sellers, J.S. Wallace, HAPEX-Sahel: a large-scale study of land–atmosphere interactions in the semi-arid tropics. Ann. Geophys. **12**(1), 53–64 (1994)

S. Halldin, S.E. Gryning, L. Gottschalk, A. Jochum, L.C. Lundin, A.A. Van de Griend, Energy, water and carbon exchange in a boreal forest landscape – NOPEX experiences. Agric. For. Meteorol. **98–99**, 5–29 (1999)

O.K. Hartogensis, H.A.R. De Bruin, Monin–Obukhov similarity functions of the structure parameter of temperature and turbulent kinetic energy dissipation rate in the stable boundary layer. Bound.-Layer Meteorol. **116**(2), 253–276 (2005)

O.K. Hartogensis, C.J. Watts, J.C. Rodriguez, H.A.R. De Bruin, Derivation of an effective height for scintillometers: La Poza experiment in northwest Mexico. J. Hydrometeorol. **4**, 915–928 (2003)

J.L. Heilman, C.L. Brittin, C.M.U. Neale, Fetch requirements for Bowen ratio measurements of latent and sensible heat fluxes. Agric. For. Meteorol. **44**, 261–273 (1989)

B. Heusinkverld, A. Jacobs, A. Holtslag, et al., Surface energy balance closure in an arid region: role of soil heat flux. Agric. For. Meteorol. **122**, 21–37 (2004)

R.J. Hill, R.A. Bohlander, S.F. Clifford, R.W. McMillan, J.T. Priestly, W.P. Schoenfeld, Turbulence-induced millimeter-wave scintillation compared with micrometeorological measurements. IEEE Trans. Geosci. Remote Sens. **26**, 330–342 (1988)

J.C.B. Hoedjes, R.M. Zuurbier, C.J. Watts, Large aperture scintillometer used over a homogeneous irrigated area, partly affected by regional advection. Bound.-Layer Meteorol. **105**, 99–117 (2002)

D.Y. Hollinger, A.D. Richardson, Uncertainty in eddy covariance measurements and its application to physiological models. Tree Physiol. **25**, 873–885 (2005)

T.W. Horst, J.C. Weil, Footprint estimation for scalar flux measurements in the atmospheric surface layer. Bound.-Layer Meteorol. **59**, 279–296 (1992)

T.A. Howell, A.D. Schneider, M.E. Jensen, History of lysimeter design and use for evapotranspiration measurements, in *Lysimeters for Evapotranspiration and Environmental Measurements*, IR Diy/ASCE/Honolulu, 23–25 July 1991, pp. 1–9

C.I. Hsieh, G. Katul, T.W. Chi, An approximate analytical model for footprint estimation of scalar fluxes in thermally stratified atmospheric flows. Adv. Water Resour. **23**(7), 765–772 (2000)

D.F. Hui, S. Wan, B. Su, G. Katul, R. Monson, Gap-filling missing data in eddy covariance measurements using multiple imputation (MI) for annual estimation. Agric. For. Meteorol. **121**(1–2), 93–111 (2004)

K.H. Jensen, T.H. Illangasekare, HOBE: a hydrological observatory. Vadose Zone J. **10**, 1–7 (2011)

Z.Z. Jia, S.M. Liu, Z.W. Xu, Y.J. Chen, M.J. Zhu, Validation of remotely sensed evapotranspiration over the Hai River Basin, China. J. Geophys. Res. **117**, D13113 (2012). https://doi.org/10.1029/2011JD017037

R. Jin, X. Li, B.P. Yan, X.H. Li, W.M. Luo, M.G. Ma, J.W. Guo, J. Kang, Z.L. Zhu, A nested eco-hydrological wireless sensor network for capturing surface heterogeneity in the middle-reach of Heihe River Basin, China. IEEE Geosci. Remote Sens. Lett. **11**(11), 2015–2019 (2014)

M. Khalil, M. Sakai, M. Mizoguchi, T. Miyazaki, Current and prospective applications of Zero Flux Plane (ZFP) method. J. Jpn. Soc. Soil Phys. **95**, 75–90 (2003)

J. Kleissl, J. Gomez, S.H. Hong, Large aperture scintillometer intercomparison study. Bound.-Layer Meteorol. **128**, 133–150 (2009)

R. Kormann, F.X. Meixner, An analytic footprint model for neutral stratification. Bound.-Layer Meteorol. **99**, 207–224 (2001)

M.R. Kuhlman, H. Loescher, R. Leonard, R. Farnsworth, T.E. Dawson, E.F. Kelly, A new engagement model to complete and operate the national ecological observatory network. Bull. Ecol. Soc. Am. **97**, 283–287 (2016)

D. Lenschow, J. Mann, L. Kristensen, How long is long enough when measuring fluxes and other turbulence statistics? J. Atmos. Ocean. Technol. **11**(3), 661–673 (1994)

X. Li, X.W. Li, Z.Y. Li, M.G. Ma, J. Wang, Q. Xiao, Q. Liu, T. Che, E.X. Chen, G.J. Yan, Z.Y. Hu, L.X. Zhang, R.Z. Chu, P.X. Su, Q.H. Liu, S.M. Liu, J.D. Wang, Z. Niu, Y. Chen, R. Jin, W.Z. Wang, Y.H. Ran, X.Z. Xin, H.Z. Ren, Watershed allied telemetry experimental research. J. Geophys. Res. **114**, D22103 (2009). https://doi.org/10.1029/2008JD011590

X. Li, G.D. Cheng, S.M. Liu, Q. Xiao, M.G. Ma, R. Jin, T. Che, Q.H. Liu, W.Z. Wang, Y. Qi, J.G. Wen, H.Y. Li, G.F. Zhu, J.W. Guo, Y.H. Ran, S.G. Wang, Z.L. Zhu, J. Zhou, X.L. Hu, Z.W. Xu, Heihe watershed allied telemetry experimental research (HiWATER): scientific objectives and experimental design. Bull. Am. Meteorol. Soc. **94**(8), 1145–1160 (2013)

C. Liebethal, B. Huwe, T. Foken, Sensitivity analysis for two ground heat flux calculation approaches. Agric. For. Meteorol. **132**, 253–262 (2005)

S.M. Liu, Z.W. Xu, W.Z. Wang, J. Bai, Z.Z. Jia, M.J. Zhu, J.M. Wang, A comparison of eddy-covariance and large aperture scintillometer measurements with respect to the energy balance closure problem. Hydrol. Earth Syst. Sci. **15**(4), 1291–1306 (2011)

S.M. Liu, Z.W. Xu, Z.L. Zhu, Z.Z. Jia, M.J. Zhu, Measurements of evapotranspiration from eddy-covariance systems and large aperture scintillometers in the Hai River Basin, China. J. Hydrol. **487**, 24–38 (2013)

S.M. Liu, Z.W. Xu, L.S. Song, Q.Y. Zhao, Y. Ge, T.R. Xu, Y.F. Ma, Z.L. Zhu, Z.Z. Jia, F. Zhang, Upscaling evapotranspiration measurements from multi-site to the satellite pixel scale over heterogeneous land surfaces. Agric. For. Meteorol. **230–231**, 97–113 (2016)

L. Lu, S.M. Liu, Z.W. Xu, J.M. Wang, X.W. Li, Results from measurements of large aperture scintillometer over different surfaces. J. Appl. Meteorol. Sci. **20**(2), 171–178 (2009) (In Chinese with English abstract)

A. Lüdi, F. Beyrich, C. Matzler, Determination of the turbulent temperature–humidity correlation from scintillometric measurements. Bound.-Layer Meteorol. **117**, 525–550 (2005)

E. Malek, G.E. Bingham, Comparison of the Bowen ratio-energy balance and the water balance methods for the measurement of evapotranspiration. J. Hydrol. **146**, 209–220 (1993)

J. Mann, D.H. Lenschow, Errors in airborne flux measurements. J. Geophys. Res. **99**(7), 14519–14526 (1994)

M. Mauder, T. Foken, R. Clement, J.A. Elbers, W. Eugster, T. GrÜnwald, B. Heusinkveld, O. Kolle, Quality control of CarboEurope flux data – part 2: inter-comparison of eddy-covariance software. Biogeosciences **5**, 451–462 (2008)

K.J. McAneney, A.E. Green, M.S. Astill, Large-aperture scintillometry – the homogeneous case. Agric. For. Meteorol. **76**, 149–162 (1995)

W.M.L. Meijninger, A.E. Green, O.K. Hartogensis, W. Kohsiek, C.B. Hoedjes, R.M. Zuurbier, H. A.R. De Bruin, Determination of area-averaged water vapour fluxes with large aperture and radio wave scintillometers over a heterogeneous surface – Flevoland field experiment. Bound.-Layer Meteorol. **105**, 63–83 (2002)

D. Michel, C. Jiménez, D.G. Miralles, M. Jung, M. Hirschi, A. Ershadi, B. Bartens, M.F. McCabe, J.B. Fisher, Q. Mu, S.I. Seneviratne, E.F. Wood, D. Fernández-Prieto, The WACMOS-ET project – part 1: tower-scale evaluation of four remote-sensing-based evapotranspiration algorithms. Hydrol. Earth Syst. Sci. **20**, 803–822 (2016)

A.F. Moene, F. Beyrich, O.K. Hartogensis, Developments in scintillometer. Bull. Am. Meteorol. Soc. **90**(5), 694–698 (2009)

J. Moncrieff, R. Clement, J. Finnigan, T. Meyers, Averaging, detrending, and filtering of eddy covariance time series, in *Handbook of Micrometeorology*, ed. by X. Lee et al. (Kluwer, Dordrecht, 2004), pp. 7–31

T. Nakai, K. Shimoyama, Ultrasonic anemometer angle of attack errors under turbulent conditions. Agric. For. Meteorol. **162–163**, 14–26 (2012)

J.O. Payero, C.M.U. Neale, J.L. Wright, R.G. Allen, Guidelines for validating Bowen ratio data. Trans. ASAE **46**(4), 1051–1060 (2003)

P.J. Perez, F. Castellvi, M. Ibañez, J.I. Rosell, Assessment of reliability of Bowen ratio method for partitioning fluxes. Agric. For. Meteorol. **97**, 141–150 (1999)

J.H. Prueger, J.L. Hatfield, J.K. Aase, J.L. Pikul Jr., Bowen-ratio comparisons with lysimetric evapotranspiration. Agron. J. **89**, 730–736 (1997)

Y.H. Qu, Y.Q. Zhu, W.C. Han, J.D. Wang, M.G. Ma, Crop leaf area index observations with a wireless sensor network and its potential for validating remote sensing products. IEEE J. Sel. Top. Appl. Earth Obs. Remote Sens. **7**(2), 431–444 (2014)

R. Ringgaard, M. Herbst, T. Friborg, K. Schelde, A.G. Thomsen, H. Soegaard, Energy fluxes above three disparate surfaces in a temperate mesoscale coastal catchment. Vadose Zone J. **11**, 54–66 (2011)

RPG Radiometer Physics GmbH, RPG-MWSC-160 microwave scintillometer manual, version 1.02. Meckenheim (2014)

H.P. Schmid, Source areas for scalars and scalar fluxes. Bound.-Layer Meteorol. **67**, 293–318 (1994)

H.P. Schmid, Experimental design for flux measurements: matching scales of observations and fluxes. Agric. For. Meteorol. **87**, 179–200 (1997)

H.P. Schmid, Footprint modeling for vegetation atmosphere exchange studies: a review and perspective. Agric. For. Meteorol. **113**, 159–183 (2002)

P. Schotanus, F.T.M. Nieuwstadt, H.A.R. De Bruin, Temperature measurement with a sonic anemometer and its application to heat and moisture fluxes. Bound.-Layer Meteorol. **26**, 81–93 (1983)

P.J. Sellers, F.G. Hall, G. Asrar, D.E. Strebel, R.E. Murphy, The first ISLSCP field experiment (FIFE). Bull. Am. Meteorol. Soc. **69**(1), 22–27 (1988)

P. Sellers, F. Hall, H. Margolis, B. Kelly, D. Baldocchi, G. Hartog, J. Cihlar, M.G. Ryan, B. Goodison, P. Crill, K.J. Ranson, D. Lettenmaier, D.E. Wickland, The boreal ecosystem–atmosphere study (BOREAS): an overview and early results from the 1994 field year. Bull. Am. Meteorol. Soc. **76**, 1549–1577 (1995)

D.I. Stannard, A theoretically based determination of Bowen-ratio fetch requirements. Bound.-Layer Meteorol. **83**, 375–406 (1997)

P.C. Stoy, M. Mauder, T. Foken, M. Barbara, E. Boegh, A. Ibrom, M.A. Arain, A. Arneth, M. Aurela, C. Bernhofer, A. Cescatti, E. Dellwik, P. Duce, D. Gianelle, E. Gorsel, G. Kiely, A. Knohl, H. Margolis, H. McCaughey, L. Merbold, L. Montagnani, D. Papale, M. Reichstein, M. Saunders, P. Serrano-Ortiz, M. Sottocornola, D. Spano, F. Vaccari, A. Varlagin, A data-driven analysis of energy balance closure across FLUXNET research sites: the role of landscape scale heterogeneity. Agric. For. Meteorol. **171–172**, 137–152 (2013)

W.C. Swinbank, The measurement of vertical transfer of heat and water vapor by eddies in the lower atmosphere. J. Meteorol. **8**, 135–145 (1951)

G.I. Taylor, The spectrum of turbulence. Proc. R. Soc. **164**(919), 476–490 (1938)

V. Thiermann, H. Grassl, The measurement of turbulent surface-layer fluxes by use of bichromatic scintillation. Bound.-Layer Meteorol. **58**, 367–389 (1992)

C.W. Thornthwaite, B. Holzman, The determination of evaporation from land and water surfaces. Mon. Weather Rev. **67**(1), 4–11 (1939)

R.W. Todd, S.R. Evett, T.A. Howell, The Bowen ratio-energy balance method for estimating latent heat flux of irrigated alfalfa evaluated in a semi-arid, advective environment. Agric. For. Meteorol. **103**, 335–348 (2000)

T.E. Twine, W.P. Kustas, J.M. Norman, D.R. Cook, P.R. Houser, T.P. Meyers, J.H. Prueger, P.J. Starks, M.L. Wesely, Correcting eddy-covariance flux underestimates over a grassland. Agric. For. Meteorol. **103**, 279–300 (2000)

H.E. Unland, P.R. Houser, W.J. Shuttleworth, Z.L. Yang, Surface flux measurement and modelling at a semi-arid Sonoran Desert site. Agric. For. Meteorol. **82**, 119–153 (1996)

S.B. Verma, N.J. Rosenberg, B.L. Blad, Turbulent exchange coefficients for sensible heat and water vapor under advective conditions. J. Appl. Meteorol. **17**, 330–338 (1978)

T.I. Wang, G.R. Ochs, S.F. Clifford, A saturation–resistant optical scintillometer to measure C_n^2. J. Opt. Soc. Am. **69**, 334–338 (1978)

J.M. Wang, J.X. Zhuang, W.Z. Wang, S.M. Liu, Z.W. Xu, Assessment of uncertainties in eddy covariance flux measurement based on intensive flux matrix of HiWATER-MUSOEXE. IEEE Geosci. Remote Sens. Lett. **12**(2), 259–263 (2015)

H.C. Ward, Scintillometry in urban and complex environments: a review. Meas. Sci. Technol. **28**, 064005 (2017). https://doi.org/10.1088/1361-6501/aa5e85

E.K. Webb, G.I. Pearman, R. Leuning, Correction of flux measurements for density effects due to heat and water vapour transfer. Q. J. R. Meteorol. Soc. **106**, 85–100 (1980)

L.A. Wever, L.B. Flanagan, P.J. Carlson, Seasonal and interannual variation in evapotranspiration, energy balance and surface conductance in a northern temperate grassland. Agric. For. Meteorol. **112**, 31–49 (2002)

J.M. Wilczak, S.P. Oncley, S.A. Stage, Sonic anemometer tilt correction algorithms. Bound.-Layer Meteorol. **99**, 127–150 (2001)

K.B. Wilson, D.D. Baldocchi, Seasonal and interannual variability of energy fluxes over a broadleaved temperate deciduous forest in North America. Agric. For. Meteorol. **100**, 1–18 (2000)

K.B. Wilson, P.J. Hanson, P.J. Mulholland, D.D. Baldocchi, S.D. Wullschleger, A comparison of methods for determining forest evapotranspiration and its components: sap-flow, soil water budget, eddy covariance and catchment water balance. Agric. For. Meteorol. **106**, 153–168 (2001)

S.D. Wullschleger, F.C. Meinzer, R.A. Vertessy, A review of whole-plant water use studies in trees. Tree Physiol. **18**, 499–512 (1998)

Z.W. Xu, S.M. Liu, X. Li, S.J. Shi, J.M. Wang, Z.L. Zhu, T.R. Xu, W.Z. Wang, M.G. Ma, Intercomparison of surface energy flux measurement systems used during the HiWATER-MUSOEXE. J. Geophys. Res. **118**, 13140–13157 (2013)

Z.W. Xu, Y.F. Ma, S.M. Liu, W.J. Shi, J.M. Wang, Assessment of the energy balance closure under advective conditions and its impact using remote sensing data. J. Appl. Meteorol. Climatol. **56**(1), 127–140 (2017)

T.R. Xu, S.M. Liu, Z.W. Xu, S.L. Liang, L. Xu, A dual-pass data assimilation scheme for estimating surface energy fluxes with FY3-AVIRR land surface temperature. Sci. China Earth Sci. **58**(2), 211–230 (2015)

K. Yang, J. Wang, A temperature prediction–correction method for estimating surface soil heat flux from soil temperature and moisture data. Science **51**(5), 721–729 (2008)

S. Zacharias, H. Bogena, L. Samaniego, M. Mauder, R. Fuβ, T. Pütz, M. Frenzel, M. Schwank, C. Baessler, K. Butterbach-Bahl, O. Bens, E. Borg, A. Brauer, P. Dietrich, I. Hajnsek, G. Helle, R. Kiese, H. Kunstmann, S. Klotz, J.C. Munch, H. Paper, E. Priesack, H.P. Schmid, R. Steinbrecher, U. Rosenbaum, G. Teutsch, H. Vereeken, A network of terrestrial environmental observatories in Germany. Vadose Zone J. **10**, 955–973 (2011)